Evaluation of Photogrammetry at Different Scales

by

Caleb Duke

A thesis submitted to the Graduate Faculty of
Auburn University
in partial fulfillment of the
requirements for the Degree of
Master of Science

Auburn, Alabama
May 5, 2018

Keywords: Photogrammetry, Structure From Motion, Stream Monitoring, Stream Morphology

Approved by

Eve Brantley, Chair, Extension Specialist & Associate Professor of Crop, Soil and Environmental Sciences
Thorsten Knappenberger, Co-Chair, Assistant Professor of Crop, Soil and Environmental Sciences
Stephanie Shepherd, Assistant Professor of Geosciences
David Blersch, Assistant Professor of Biosystems Engineering

Abstract

Accelerated erosion is amplified by anthropogenic effects, which can lead to changes in stream geometry. Stream topography measurements over time quantify stream bank erosion. The goals of this project are to evaluate topographic survey methods for costs, effort, and accuracy; to develop a stream geometry monitoring method based on photogrammetry; and to evaluate stream channel adjustment from post restoration. The objectives are to study the influence of vegetation on accuracy of a photogrammetric model, compare photogrammetric surveys to total station surveys and to evaluate replication over time using photogrammetric surveys.

Photogrammetry is a measurement technique that creates 3D surface models from multiple images. Structure-from-motion (SFM) is a type of photogrammetry where ground control points are required and can be simplified through automation. SFM was used throughout this study for model evaluation. Photogrammetry accuracy depends on image quality, number of images, image angle, and obscurity by object such as vegetation. Lab and field experiments were conducted to examine these parameters. Volume models created from a 23.0cm x 20.5cm x 16.5cm box were evaluated. Treatments included two cameras, a digital single lens reflex (DSLR) and cell phone Samsung Galaxy S4; change in camera angles, and vegetation density (ornamental English ivy). A volume model was considered accurate when it matched at least 95% of the box volume. Models with no vegetation were accurate with a minimum of 21 images from both the Samsung Galaxy S4 and DSLR.

Model error increased and accuracy diminished with fewer images. Models accuracy decreased when less than 21 images were used to develop models of the box alone and the box with vegetation. Vegetation density was evaluated based on leaf area index (LAI) and

a vegetation obscurity index. Model error was greater than 5% at an LAI above 0.07 and a vegetation obscurity of 7%.

Field studies with two truncated soil pyramids (1m x 1m and 2m x 2m) planted with German millet were evaluated for volume accuracy. Twenty-four images were captured for the small pyramid and 40 for the large pyramid to ensure proper overlap among images with the cell phone and DSLR. Image sets were taken weekly from week zero (no vegetation) to week four (100% vegetation cover). At week zero both pyramids had 1.5% error (or greater) with both cameras, and at week four there was 100% error with both cameras. There is a positive relationship between increasing vegetation density and model error.

A stream restoration site on Parkerson Mill Creek was evaluated over time for post-construction channel morphology adjustment to further evaluate the impact of vegetation on photogrammetric model accuracy. Ground control points were installed to determine stream geometry change (i.e. erosion or deposition). A base line study comparing total station transects to digital elevation models from photogrammetry show that SFM photogrammetry is an accurate method to evaluate stream geometry. A second study was conducted to determine change over time or channel evolution within DEMs. The average root mean square error for the survey comparison is less than 1m. We conclude that SFM photogrammetry taken from ground control points at stream level by a Samsung Galaxy S4 and DSLR camera may be useful as a tool to monitor stream geometry change over time. Similar points within each of the models had an RMSE of less than 1.2m. Models accuracy may have been diminished by vegetation density or shading, field of view, and placement of ground control points.

Acknowledgments

Foremost, I would like to express my sincere gratitude to my advisors Dr. Eve Brantley and Dr. Thorsten Knappenberger for the continuous support of my M.S. study and research, for their patience, motivation, enthusiasm, and immense knowledge. Their guidance was invaluable during both the research and writing of this thesis.

I would also like to thank the rest of my thesis committee: Dr. Stephanie Shepherd and Dr. David Blersch for their encouragement, insightful comments, and guidance.

I would like to thank my fellow labmates in the Crop, Soil and Environmental Sciences Department including, Hallie Douglas, Pan Wang, Noah Hull, Luke Carter and Aurelie Poncet for the stimulating discussions, sleepless nights we were working together before deadlines, and for all of the fun we have had in the last two years.

I would also like to give a special thanks to my wife Nikki, for her support when I needed it the most and encouragement to keep me focused.

Last but not least, I would like to thank my parents Jeff and Sandy Duke, for giving birth to me and supporting me spiritually and mentally throughout my life.

Table of Contents

List of Figures

List of Tables

Chapter 1

Introduction

Stream health includes biological, chemical and physical aspects of stream systems. Increases in urbanization are linked to degradation, altered hydrology, and increased sediment loads in stream systems (Meyer.J.L, 2005). Many of these stream systems are no longer hydrologically connected to their floodplains due to stream incision. Geologic, climatic, vegetative, and hydraulic factors are the core influences of stream bank erosion (NRCS, 2010). Stormwater is rainwater run off from impervious constructed surfaces such as driveways and rooftops. Increases in runoff from impervious surfaces associated with urbanization, such as driveways and rooftops, are linked to altered hydrology that contributes to stream bank erosion (NRCS, 2008). A stream is considered in dynamic equilibrium when it is able to maintain stability even as it adjusts in width, depth, and laterally through its valley to maintain its least erosive form (LaFlamme, 2011). Endreny (2016) states that "Stream equilibrium is a method for classifying the status of a system between aggradation (increased deposition) and degradation (increased erosion), which extends beyond the standard range of erosion and deposition of sediment."

Stream restoration may be required to assist a degraded stream in recovering functions (i.e floodplain interactions, movement of water, and treatment of pollutants). More than 37,000 stream projects have been documented and of those only 38% have been properly monitored (i.e bio-assessments, water quality) throughout the U.S. Seventy percent of projects not monitored were failing in some aspect (Bernhardt et al., 2005; Conniff, 2014; Gloss and Bernhardt., 2007). Monitoring stream restoration projects is crucial to understanding in-stream processes to evaluate long-term success. The goal of this research is to compare topographic survey methods and to evaluate photogrammetry as a cost-effective

method to document stream geometry. I hypothesize that digital terrain models from photogrammetry are similar in quality to models from traditional transect surveys and therefore can be used to document and evaluate stream restoration projects.

Monitoring stream changes in geometry over time provides information on channel adjustment, including streambank erosion. There are several techniques to measure stream geometry, including transect survey, ground base LIDAR (Light Detection and Ranging, 3D laser scanning), and photogrammetry. Using cross sections as an example, a transect survey is an inexpensive method to measure the channel dimensions, but it is time consuming and represents the channel geometry in only two dimensions. 3D surface models can be created with ground-based LIDAR; however, the instrument is expensive and requires expert knowledge. An alternative monitoring method is photogrammetry which creates 3D models from images. Compared to transect surveys and ground-based LIDAR, photogrammetry is an easy to use, low-cost method to create accurate 3D surface models (Hooke., 1997; Javernick et al., 2014).

1.1 Stream Geometry

Stream geometry is based on water movement, channel width, channel depth, water velocity, and water volume to a discharge area (Leopold and Maddock, 1953; Merigliano, 1997). Stream geometry is measurements of a hydraulic system to define the shape of a stream channel. Measurements of stream geometry include channel depth, channel width, water velocity and suspended load (Australia, 2016; NRCS, 2010). Channel width and depth make up the cross-sectional area of the stream and define access to the floodplain (Leopold and Maddock, 1953). Geomorphology of streams tends to be symmetrical in the shape of semielliptical, trapezoidal, or triangular, and when discharge is increased these shapes are manipulated due to change in flow patterns (Leopold and Maddock, 1953). A stream will shift in morphology to manage the energy of flow and sustain functionality (Clarified, 2003). Sear (1994) describes a stream channel as the conduit for water being carried by

the stream, constantly adjusting its shape and slope in relation to the water it may carry at a given time. Stream geometry influences several functions including bank stability, vegetation growth, wildlife habitat, water quality, and soil and water interactions. Soil and water are two factors that influence stream geometry. Soils will vary over topography and geological location; different soil structure and textures will have different erosive potential. Stream channel processes such as sediment transport are important for understanding the link between morphological changes within a stream (Lane, 2000).

Classification schemes are useful to communicate stream geometry, to aid in the understanding of stream condition and potential response under the influence of different types of changes. The Rosgen (1994) classification scheme sorts streams into categories of stream types and subtypes (Figure **??**). The broad stream types are based on landscape and stream geometry. Streams are classified as A-G and the subtypes are based on slope ranges. Other factors include the channel substrate particle size.

Lane (2000) states that a move away from stable hydraulic geometry alters the channel and increases the importance on documenting morphological measurements. Lane suggests the following steps are needed when analyzing stream geometry measurements:

1. Evaluate and understand stream channel changes,

2. Measure deposition and erosion, and

3. Collect data for input into 2D and 3D models of stream channel processes.

These steps are crucial for collecting information on a stream and how it may respond to outside pressures. Data collection is a crucial step in understanding how a stream responds to changes. Streams are dynamic therefore stream geometry measurements must be monitored to better predict how a stream may respond to change.

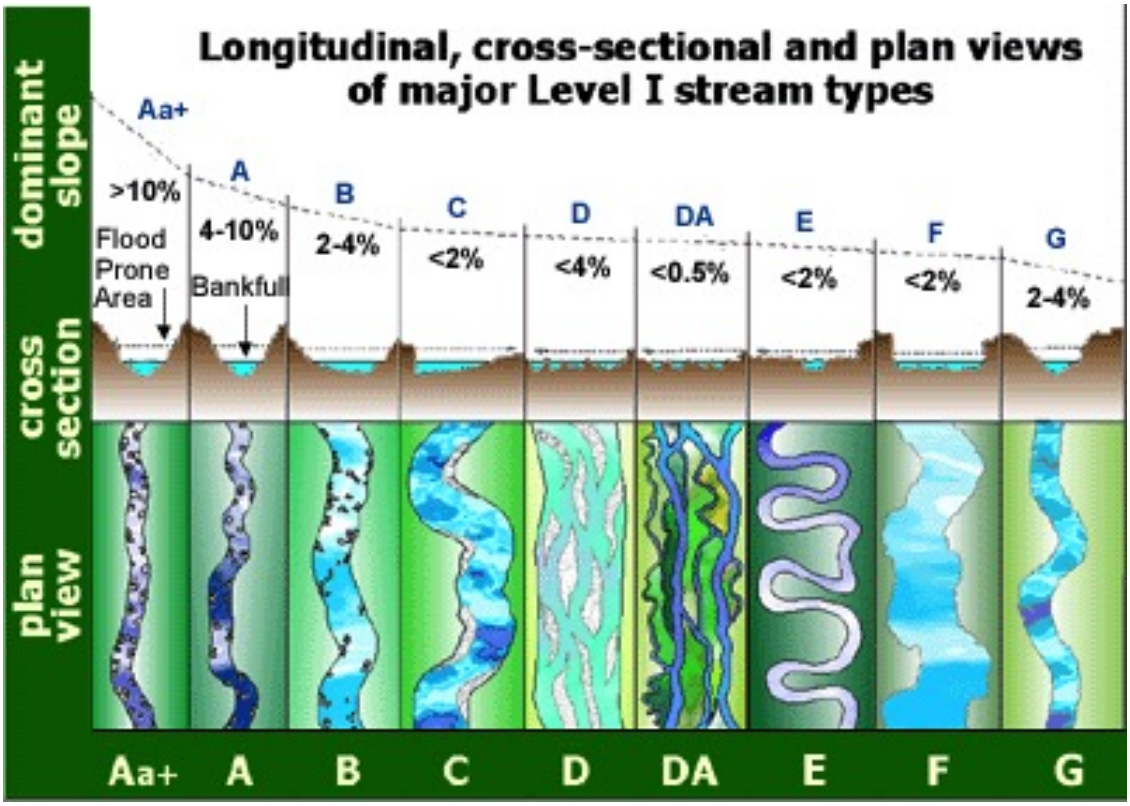

Figure 1.1: Rosgen stream classification: This diagram compares the longitudinal, cross-sectional, and plan views of each of the nine major stream types in the Level I classification (Rosgen,1994).

1.2 Techniques for Surveying Stream Geometry

Technologies, such as LIDAR, photogrammetry, and total station, have expanded the tools for evaluating stream geometric change. These emerging technologies have advanced the ability to monitor stream geometric change through georeference and 3D capabilities (Bird et al., 2010). This advancement in technology has influenced conventional total station survey by increasing accuracy through direct georeference survey. Indirect georeference methods, or photogrammetric methods, improve accuracy and efficiency in fields such as geomorphology and forestry (Scherer and Luis Lerma, 2009). 3D technologies (i.e., LIDAR, photogrammetry) have been noted to detect changes in stream geometry at high accuracy (Dietrich, 2016; Westoby et al., 2012).

1.2.1 Total Station/Transect Survey

Total station theodolite (total station) surveys are a common survey technique that creates 2D representations of an object. The total station can be used to measure exact point locations and to link points over space to measure stream geometry. A total station collects data electronically, while incorporating an electronic distance-measuring device that eliminates the need for manual measurements; the device allows rapid measurements with greater accuracy than traditional range finders and eye levels (Keim et al., 1999). The United States Geological Survey (USGS), and the United States Environmental Protection Agency (EPA) both use transect-based surveys, also considered ground survey methods, to conduct stream surveys (Ballow, 2016).

Keim et al. (1999), describes quantification of channel morphology as a necessity for sub-disciplines within the fluvial sciences. The collection of data from a two-dimensional survey method such as total station allows for sufficient data to link hydrology and stream morphology (Keim et al., 1999). Total stations are adequate to measure channel depth, width and slope measurements. Each cross section comprises point measurements that quantify distance, elevation, and slope change across the stream, thus allowing for determination

of stream geometry (Haney and Davis, 2015). However, topographic surveys can be labor intensive and produce large data sets as well as extensive monitoring periods (De Santisteban et al., 2006). The 2D data produced by total stations can be interpolated into 3D digital elevation models. 3D models are the most useful information in channel morphology studies (Keim et al., 1999).

Total station surveys require two people for data collection: the rod-man (person holding the measuring rod) and the person running the theodolite (Armistead, 2013). Total station is also an expensive survey method ranging from $3,000 to $15,000 (Topcon, 2017). A total station survey also requires more man hours than other technologies such as photogrammetry; This study required 18 total man hours to complete one total station survey, while the photogrammetry survey required approximately 3 hours per survey.

1.2.2 Traditional Photogrammetry

Traditional photogrammetry now referred to as photogrammetry is the art, science and technology of producing 3D models of land surfaces (Samad et al., 2010). Photogrammetry is based on images to quantify measurements of a scene to be studied (McGlone and Lee, 2013; Schindler, 2016). Photogrammetric surveys are conducted using cameras such as cell phones, digital single lens reflex (DSLR) cameras, and unmanned aerial vehicles (UAV). Image quality differs between camera types, which may require more images to be taken per device (Photomodeler, 2016). Photogrammetry is noted to be as accurate or more accurate than traditional survey methods while being much more cost effective (Armistead, 2013; Dietrich, 2016).

Photogrammetry has advanced the traditional survey of geomorphological terrain analysis to 3D hydrographic surveys. Photogrammetry can be used with total station surveys or as a stand-alone tool. Photogrammetry surveys are cost efficient and can be high quality (Westoby et al., 2012). These surveys have been used in geomorphology for monitoring changes in streams over time (Lane et al., 1994; Westoby et al., 2012).

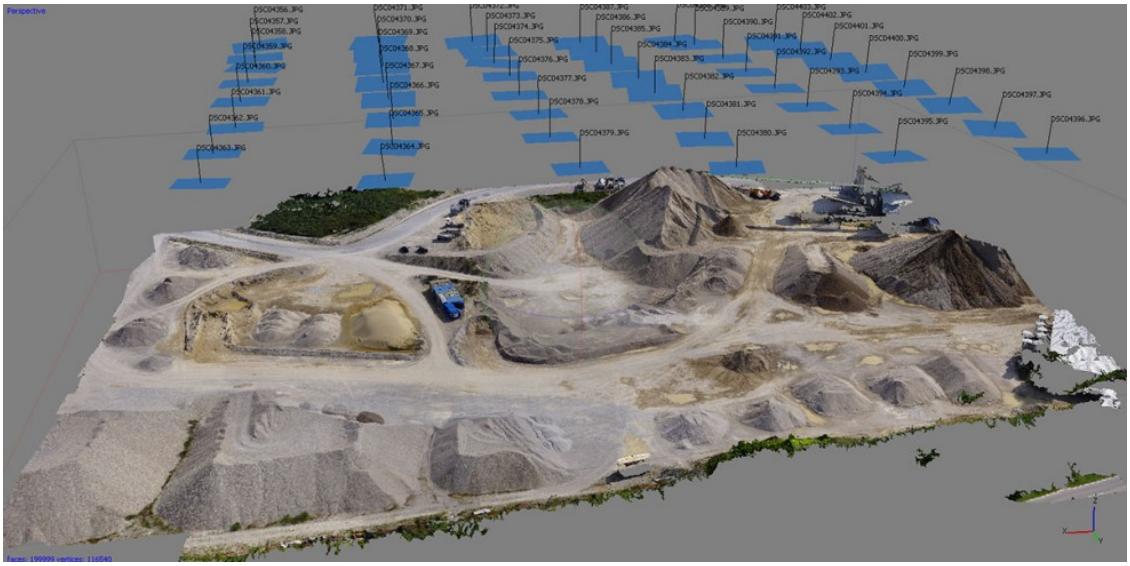

Figure 1.2: Example of UAV aerial photogrammetry image capture processed in the Agisoft Photoscan (Celestis.de).

Photogrammetry consists of two techniques, close-range photogrammetry and aerial photogrammetry. Close-range photogrammetry is defined as photographs taken within 300m of a test subject. These images are captured with the use of a DSLR or cell phone. Close-range photogrammetry is considered non-topographic; that is, the output is not like terrain models or topographic maps, but instead produces 3D models which are measurements and point clouds capable of producing digital elevation models (ASPRS, 2016). Aerial photogrammetry is conducted by aircraft with an attached camera to capture images from the air. This type of photogrammetry uses specified flight patterns to fly and capture images (Figure 1.2). Aerial photogrammetry produced accurate models of fluvial geomorphology in relation to other survey techniques (Armistead, 2013; Baptiste et al., 2016).

Photogrammetry uses multiple images overlapped to solve the trigonometry of the data collected (Dietrich, 2016). In traditional photogrammetry, image matching is processed based on stereo-pairs, where software used requires parallel images at 60% overlap (James and Robson, 2012). Also, traditional photogrammetry requires control points to be recognizable in images. The location of the points must be known for accurate data analysis to produce the 3D model (Ballow, 2016).

Calibration within photogrammetry is important for creating accurate models. A reliable calibration technique includes controlled scenarios in a laboratory. Indoor reconstruction of household objects aids in understanding the process of 3D model reconstruction, which allows for proper calibration (Dikovski et al., 2016). Dikovski et al. (2016) concluded that even with lower resolution cameras it is possible to recreate high quality 3D models using photogrammetry in an indoor setting; however, using a higher quality camera will create a higher quality model. Another way to increase accuracy is to increase the number of images taken per object, creating a higher resolution point cloud (Agisoft, 2016). Once a model has been calibrated, both laboratory and field models can be accurately developed with photogrammetry (Westoby et al., 2012).

Photogrammetry can be used to model various objects from small to large (Debevec, 1996; Dikovski et al., 2016). Figure 1.3 shows small scale photo capture and Figure 1.4 shows photo capture for large-scale reconstruction. Correct photo-capture depends on the scale of an object to be modeled and it is important for 3D reconstruction and model accuracy.

Photogrammetry has been used as a measurement tool for objects including humans, buildings, and streams. Close-range photogrammetry has been used in historical studies, archeological studies, and most recently geomorphological research. Within the last 30 years photogrammetry has been used to survey geomorphology, for slope stability, coastal studies (Kidson and Manton, 1973), and river channel studies (Lane et al., 1994, 1993).

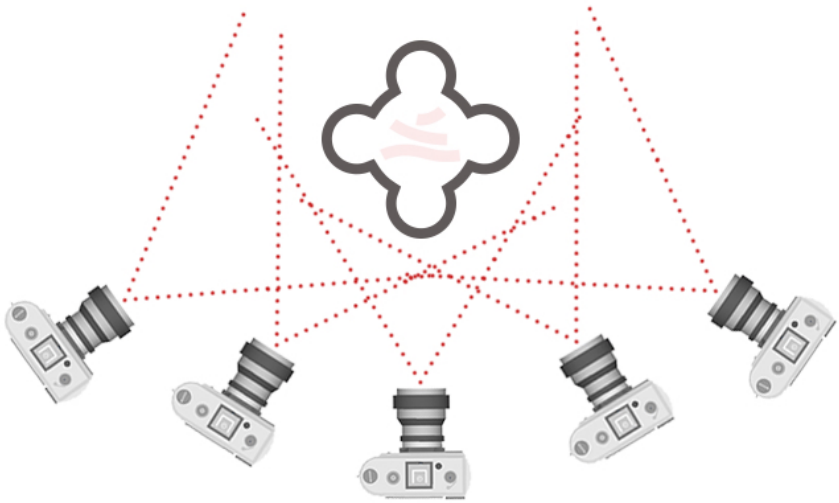

Figure 1.3: Image capture technique for small scale 3D reconstruction (3dflow.net).

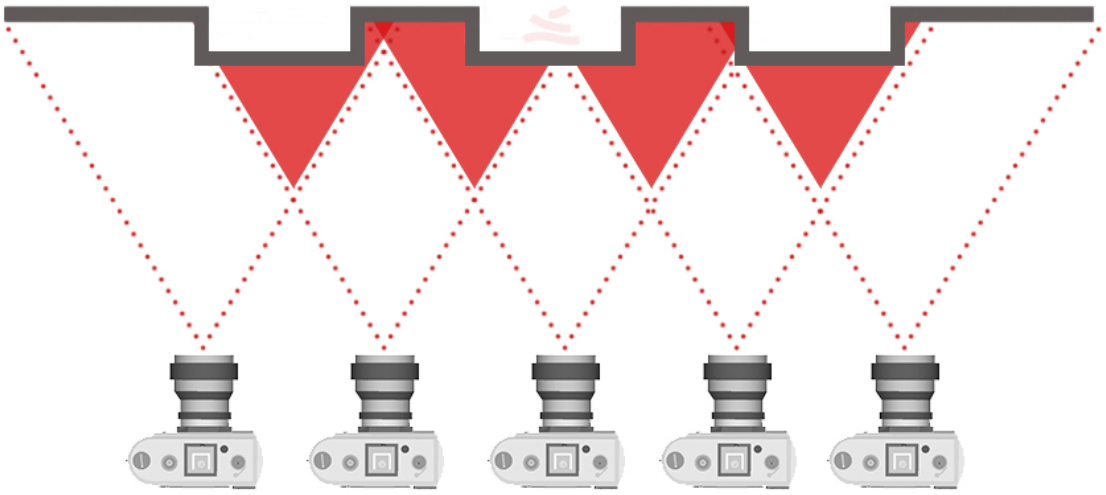

Figure 1.4: Image capture technique for large scale linear 3D reconstruction (3dflow.net).

Close-range photogrammetry includes the use of cell phones or digital cameras. Cell phones are relatively inexpensive and require less expertise to control. Because they have built-in sensors, cell phones are able to collect 3D locations and high-resolution images (Kim et al., 2013). Cell phones are ubiqutious and freely available to the research community (Micheletti et al., 2015). Mapping with mobile devices improves accuracy when calibrated, is as accurate as metric cameras, and saves time and money (Lee et al., 2012). Fawzy (2015) concluded that cell phones used in close-range photogrammetry are: (i) efficient, (ii) fast and useful, (iii) have high accuracy when compared to high-resolution cameras, and (iv) have increasing coordinates as resolution increases. Other studies have concluded that cell phones are sufficiently accurate for projects that do not require a high accuracy, although with the advancement of technologies in cell phones their cameras could be capable of producing high-resolution models (Ebrahim, 2004; Satchet, 2011). Research shows that results are similar between cell phones and true with digital cameras (DSLR). Digital cameras are capable of producing high quality models while being cost efficient and time efficient (Blizard, 2014). Differences between digital cameras and cell phones include availability and image quality. Generally, cell phones are more commonly accessible than DSLR. While both cameras take high quality images, the image formats are different. A cell phone captures a compressed image (JPEG), while the DSLR captures a RAW uncompressed image. Compression of a photo reduces quality.

Aerial photogrammetry has been used for studies including stream surveys, vegetation profiles, and erosion and sediment control. Perez et al. (2015) and Gómez-Gutiérrez et al. (2014) studied the use of UAV technology in erosion and sediment control and found it a more feasible method for monitoring practices on construction sites compared to walking the sites. UAV photogrammetry is an accurate tool for monitoring vegetation with thermal imaging, where thermal imagery allows for higher spatial resolution to recognize vegetation stress (Berni et al., 2009). Aerial photogrammetry is accurate and capable of surveying large areas quickly to create a 3D model (Bemis et.al 2014). UAVs have the potential to reduce

the error within a model that may contain gaps. Furthermore, UAVs have the capability to create high resolution topographic imagery (Javernick et al., 2014; Westoby et al., 2012). The use of an UAV may fill the gap between manned aerial photogrammetry and traditional land survey techniques (Perez et al., 2015). However, UAV technology can be expensive and may require special permits due to regulations. UAV survey areas are limited due to flight restrictions such as trees, buildings, and power-lines.

1.2.3 Structure-From-Motion Photogrammetry

Structure-from-motion (SFM) is an alternative method to traditional photogrammetry. The advancements in SFM are based on traditional photogrammetry (Dietrich, 2016). Both methods rely on image capture having multiple views. Multiple-view photogrammetry is a relatively new term defined by points recognized in multiple images for a more automated spatial reconstruction. Likewise both methods rely on the images captured to resolve 3D geometry of an object or surface (Fonstad et al., 2013). SFM differs from traditional photogrammetry in that it uses more vigorous point matching algorithms to stitch together images that usually need less overlap (Dietrich, 2016; Westoby et al., 2012). SFM is relatively simpler than traditional photogrammetry due to the algorithms' automated calculation of geometry of a scene, and the camera's orientations and position (Ballow, 2016). Micheletti et al. (2015) used SFM to document geomorphic change on a stream bank that allowed for automatically adjusting image relations, which is used to solve interior and exterior parameters of the surface model to be produced. The amount of images needed for scene re-creation varies depending on size and detail of the scene itself. For example, to re-create scenes of great detail with SFM it is important to capture the whole scene first before adjusting distance among images to ensure the scene of interest is captured. The wide range of photo directions helps create a data set, which generates a strong, accurate, precise model with the camera locations, thus giving a coordinate system (Micheletti et al., 2015).

SFM photogrammetry is widely used in studies of geomorphology and most recently used as a tool for fluvial morphology. However, there is a lack of information in the area of stream and river restoration. It is important to understand physical characteristics of habitat conditions to evaluate pre- and post-restoration success (Baptiste et al., 2016) and SFM technology can make collecting these data simple and effective.

1.2.4 Accuracy and Precision of Models

Accuracy refers to how close a measured value is to a standard or known value, and precision refers to the closeness of those measured points to one another (Figure 1.5) (Hargreaves, 2017). The terminology is independent of one another, and accuracy was used throughout this study. Typically the acceptable margin of error for research falls between 4 and 8% at the 95% confidence level for scientific studies (DataStar, 2008). An acceptable SFM range of accuracy for models will have less than 5% error or less than 1m; that is, any model having greater than 5% error or 1m will be considered inaccurate (Westoby et al., 2012). Accuracy among models is application dependent. For each study, accuracy is an application of measurement to the error of a model when compared to the known measurement. Accuracy, precision, and percent error are all dependent on the application and are designated by the user. For the following studies models created with SFM will have less than 5 percent error in a controlled setting and 1m error in field settings.

1.3 Vegetation Influence on Photogrammetry Accuracy

Stream restoration success includes establishment of riparian vegetation for long-term stability of the stream geometry. Vegetation has been shown to obscure stream geometry assessment by photogrammetric methods (Lane, 2000). Vegetation can create noise (obscurities) in models that results in error. If vegetation is present and uniform, then parameters from the digital elevation model (DEM) would not be affected (Dietrich, 2016; Fonstad et al.,

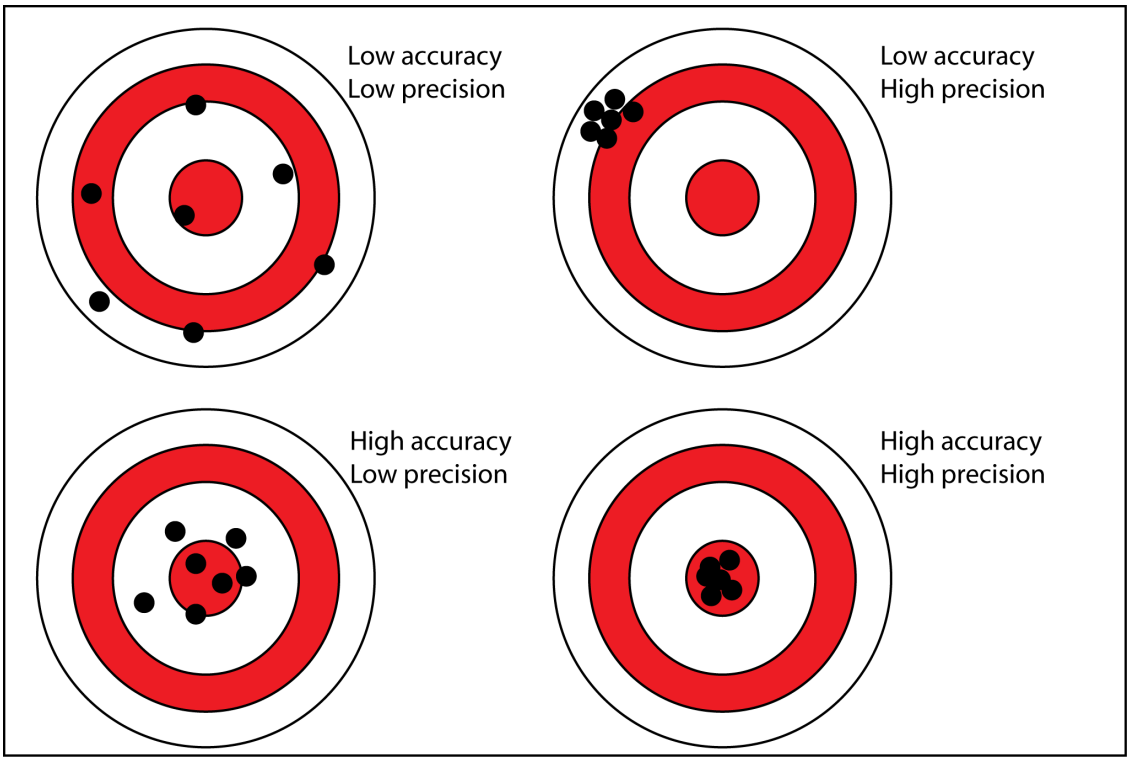

Figure 1.5: Comparison of accuracy and precision. Accurate measurements fall in the bulls eye. Precise measurements are clustered. Accurate and precise measurements are close to one another and in the bulls eye. (Williams, 2017).

2013; Lane et al., 1993; Lane, 2000). If the vegetation is of low density, then DEM construction of a stream may be possible with image classification. Inversely, high-density vegetation may limit the use of photogrammetry.

Image classification can be used to correct obscurity if the vegetation is uniformly distributed (Lane, 2000). Unfortunately, these scenarios without vegetation are not always available; therefore vegetation leads to a majority of error within photogrammetric models (Lane, 2000; Westoby et al., 2012). The best time to acquire images for optimal density of data collection for pre-processing with SFM is during low growth periods (Lane et al., 1993, 1994; Lane, 2000). Sparse vegetation within dormant seasons allows for more accurate data collection through noise reduction (Javernick et al., 2014). Fonstad et al. (2013) suggest that photogrammetry does not detect the ground beneath vegetation unless there are gaps within the canopy. Collaboration of aerial photogrammetry and close-range photogrammetry could negate the effect of vegetation within models due to more images from many viewpoints (Westoby et al., 2012; Fonstad et al., 2013).

1.4 Leaf Area Index (LAI)

Leaf area index (LAI) is defined as the one-sided leaf area per unit ground surface area and is used to measure the amount of leaf material in an ecosystem (the amount of canopy). It is also dimensionless (LAI = leaf area / ground area), and imposes important controls on photosynthesis, respiration, rain interception, and other processes (Chen and Black, 1992; McCree and Troughton, 1966; JMO, 2001). However, depending on the type of measurement, the definition of LAI as a dimensionless quantity varies (Baldocchi, 2012; Bréda, 2003). Leaf area index may be calculated with either of two approaches, the planimetric approach or gravimetric approach. The planimetric approach, used for this study, correlates between the individual leaf area and the areas covered by that leaf in a horizontal plane (Weiss and Baret, 2016). The gravimetric approach for LAI calculation is based on the correlation between

dry weight of leaves and leaf area using predetermined leaf mass per area (Weiss and Baret, 2016). Leaf area index is typically based on broad-leaf canopies.

Yan et al. (2016) and Pandey and Singh (2011), recommended that the area of a leaf should be determined by drawing a its outline on paper and measuring the enclosed area. This method is called to the graph paper method. Each leaf must be traced on the graph paper and the area the leaf covers is the surface area of that leaf. Once each leaf is measured the total area of the surface it covers is referred to as its LAI.

1.5 Stream Restoration

Stream restoration is defined as manipulating a stream to move a system toward dynamic equilibrium (Doll et al., 2003). Successful restoration requires understanding of the stream ecosystem and watershed characteristics (Copeland et al., 2001; NRCS, 2010). Stream channel evolution is influenced by hydrological dynamics and is time dependent. Streams evolve naturally as described by Schumm and Watson (1984) with the following steps: degradation, degradation and widening, aggradation and widening, and quasi-equilibrium (Figure 1.6).

Channel evolution may be used as a guide for stream restoration to develop site-specific success criteria (Booth and Fischenich, 2015). The National River Restoration Synthesis Study found that more than half of stream restoration projects in the United States fail to meet some goal (e.g., habitat improvement, water quality, or stream stability). There is a rise nationally and internationally for holistic restoration efforts that better address the primary cause of ecosystem degradation (Beechie et al., 2010).

Pess et al. (2003) and Beechie et al. (2010) describe stream restoration as process-based intervention that aims to reestablish normal rates and magnitudes of physical, chemical, and biological processes to create and sustain river and floodplain ecosystems. Processes include erosion, sediment transport, and hydrologic routing. Process-based restoration focuses on anthropogenic disturbances on these processes to determine the river to floodplain ecosystem progression over time to determine recovery time of a system with minimal corrective

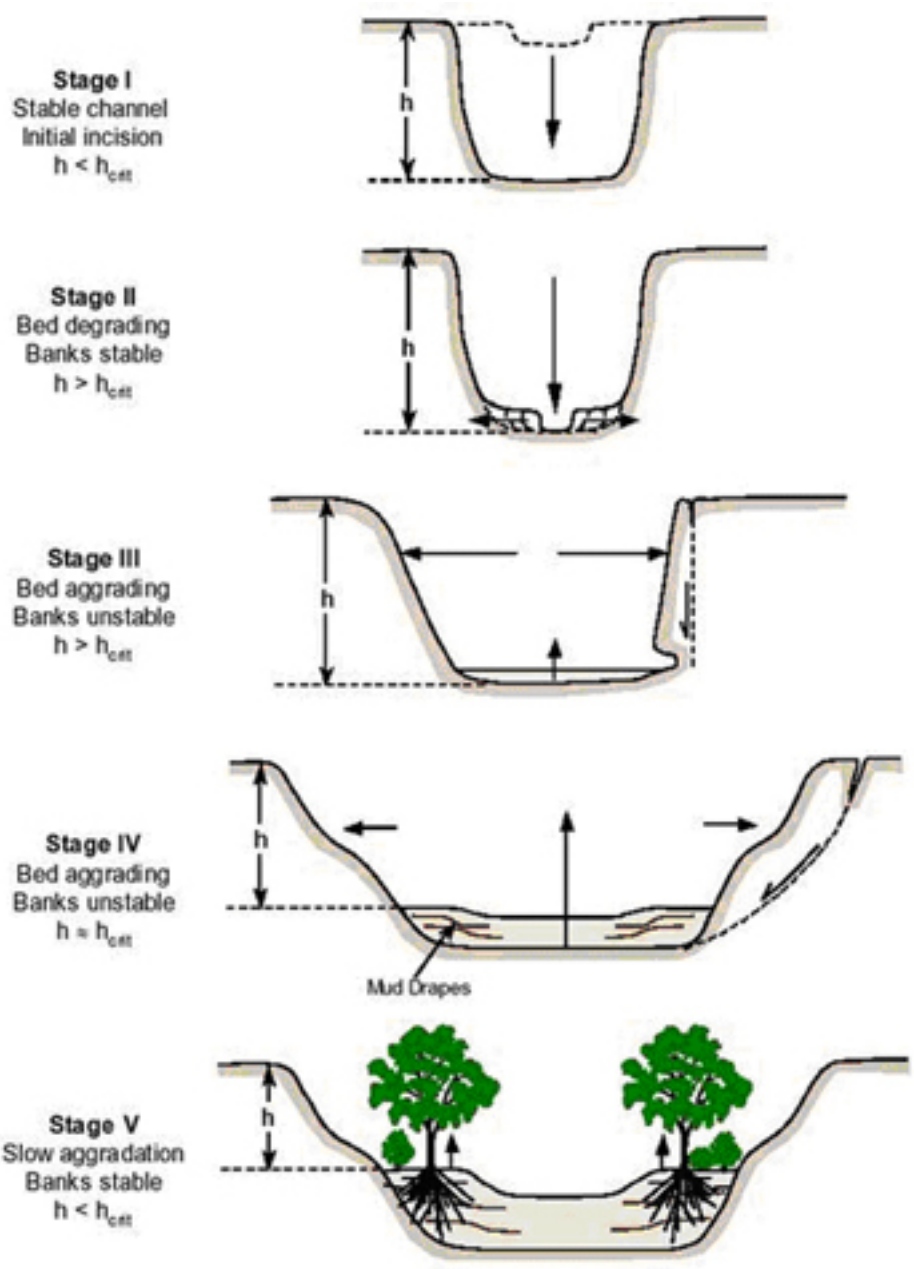

Figure 1.6: The six stage channel evolution model to explains how streams naturally shift to reach a steady state (Schumm 1984).

action (Sear, 1994). Survey techniques can be used to verify and monitor stream restoration geometry. Stream restoration design may focus on mitigation for either habitat change or morphology, or both.

Clewell et al. (2000) describes ecological restoration as the process of assisting the recovery of an ecosystem that has been degraded or destroyed. Extreme hydrological events such as floods and droughts create shifts in biological diversity and stream morphology. Long-term monitoring of stream restoration assists in understanding influences of extreme hydrological events on the overall ecological structure of streams to increase success within restoration (Lake, 2001; Reich and Lake, 2015). Small-scale restoration may show success early; however, larger restoration projects may take time (up to 7 years) to show that they are successful (Wiens, 1989).

Monitoring is crucial for the success of stream restoration and improved stream management. There is a need for better, quicker, and inexpensive, yet effective, methods of monitoring. Funding and responsibility for monitoring often falls on the shoulders of the local land managers rather than the researchers or the stream restoration professionals.

1.6 Summary

This thesis examines SFM photogrammetry as an alternative method for quantifying stream geometry. SFM photogrammetry is capable of producing high quality 3D models in less time, and may be more cost efficient than alternative methods such as total station surveys. SFM is a simple technique using images collected to reproduce 3D models for measurement. The Agisoft Photoscan software is capable of creating dense point cloud models by aligning images spatially and stitching them together. Image locations are not necessary for SFM as for traditional photogrammetry, as long as the images are of high quality and there is significant overlap. SFM could provide a valuable option for monitoring stream geometry. In this project I evaluated SFM photogrammetry based on the following

parameters: object size, number of images, vegetation effect, and comparison with total station.

The emerging technologies of high-resolution cameras at low cost can create high spatial 3D surface maps. Advances in cell phone technology have made it a feasible method for surveying stream geometry. When compared to other more expensive traditional survey techniques, cell-phone photogrammetry is a more effective method for creating surface terrain models (Matthews, 2008). The accuracy of photogrammetry is based on the quality of the images, the number of images from different angles, and amount of vegetation. Evaluation of these parameters will allow for understanding of the capabilities and constraints of photogrammetry as a method to evaluate objects of different size.

Stream restoration projects require long-term monitoring to evaluate success. Effective monitoring should be regular, long term, and inclusive of biological, physical, and chemical measurements to aid in restoration success (Erwin and Hamilton, 2005). A method such as SFM may provide effective monitoring efforts at low cost and effort. Dietrich (2016) studied the accuracy of photogrammetry as a cost effective tool to use for surface reconstruction of rivers at various scales.

The goal of my research is to compare topographic survey methods and to evaluate photogrammetry as a cost-effective method to document stream geometry and calculate stream bank erosion. The following research goals were evaluated:

1. Evaluate topographic survey methods for costs, effort, and accuracy.

2. Develop a stream geometry monitoring method based on photogrammetry.

The objectives of my research are:

1. Study the influence of vegetation on accuracy of a photogrammetric model.

2. Compare photogrammetric surveys to total station surveys.

3. Evaluate replication (accuracy over time) using photogrammetric surveys.

Chapter 2

Materials and Methods

2.1 Study Overview and Site Selection

Photogrammetric data was collected at three spatial scales: box lab study, soil pyramid field study, and stream field evaluations. Lab studies took place at Auburn University, in Auburn, Alabama. Field studies were conducted at the Auburn University Turf Grass Unit and Parkerson Mill Creek in Auburn, Alabama.

Photogrammetry was used in this study as a tool to survey and measure objects. Photogrammetry determines 3D location of images captured while connecting images from different vantage points or angles (Westoby et al., 2012). Each study evaluated photogrammetry as a tool to quantify key factors such as time, effort and accuracy. Studies were selected based on size, small scale to large scale (half meter to 100 meter) and controlled vs. non-controlled experiments (lab and field).

2.2 3D Point Cloud Dataset and Pre-Processing

Agisoft Photoscan Professional Edition was selected based on relatively low cost, ease of use, and accuracy in spatial reconstruction with limited camera information. Agisoft Photoscan has been used in geomorphology studies with success building 3D surface models from few images (Armistead, 2013; Javernick et al., 2014; Westoby et al., 2012). Agisoft Photoscan is user friendly and straightforward, allowing ease of data processing and creation of high quality models from images.

Agisoft Photoscan was used for creating point clouds from photographs that were taken using the Nikon D90 DSLR and Samsung Galaxy S4. Images were captured based on recommended methods from Agisoft Photoscan (Figure 2.1). Agisoft Photoscan is automated and requires little user input for geo-referencing and quality of each workflow processes to create the point cloud dataset and 3D model.

A batch process through the workflow option in Agisoft Photoscan was used for each model. The following procedure was used as a base for 3D model generation: align images, optimize alignment, build dense point cloud, build mesh, build texture and detect markers. Each of these steps were set on medium which is the recommended setting through the Agisoft Photoscan manual 2016. Once each of these processes has been completed a 3D model was meshed from the images input into the software.

The second procedure is to analyze the model. When analyzing a model there are several steps that are required such as recognition of control points, deletion of "noise," addition of scale bars for measurement, closing holes within the model, and measuring area and volume of the model (Figure 2.3).

For the box and pyramid study accuracy is based on a measured volume calculated through Agisoft Photoscan to a known volume. Accuracy for the stream study is calculated using the difference between a point from a digital elevation model (DEM) compared to reference point from total station data. A secondary method was used for the stream study to compare surveys over time to determine elevation change.

2.3 Controlled Studies/ Workflow

The box study and pyramid study each had an object of study, coded targets, and minimum number of required images for pre-processing through Agisoft Photoscan. For both studies, the following variables were established: vegetation, image capture (Figure 1.3), lighting, control points, and scale bars. Additionally, the volume of the small box and the pyramids was measured prior to evaluation through Agisoft Photoscan. To determine

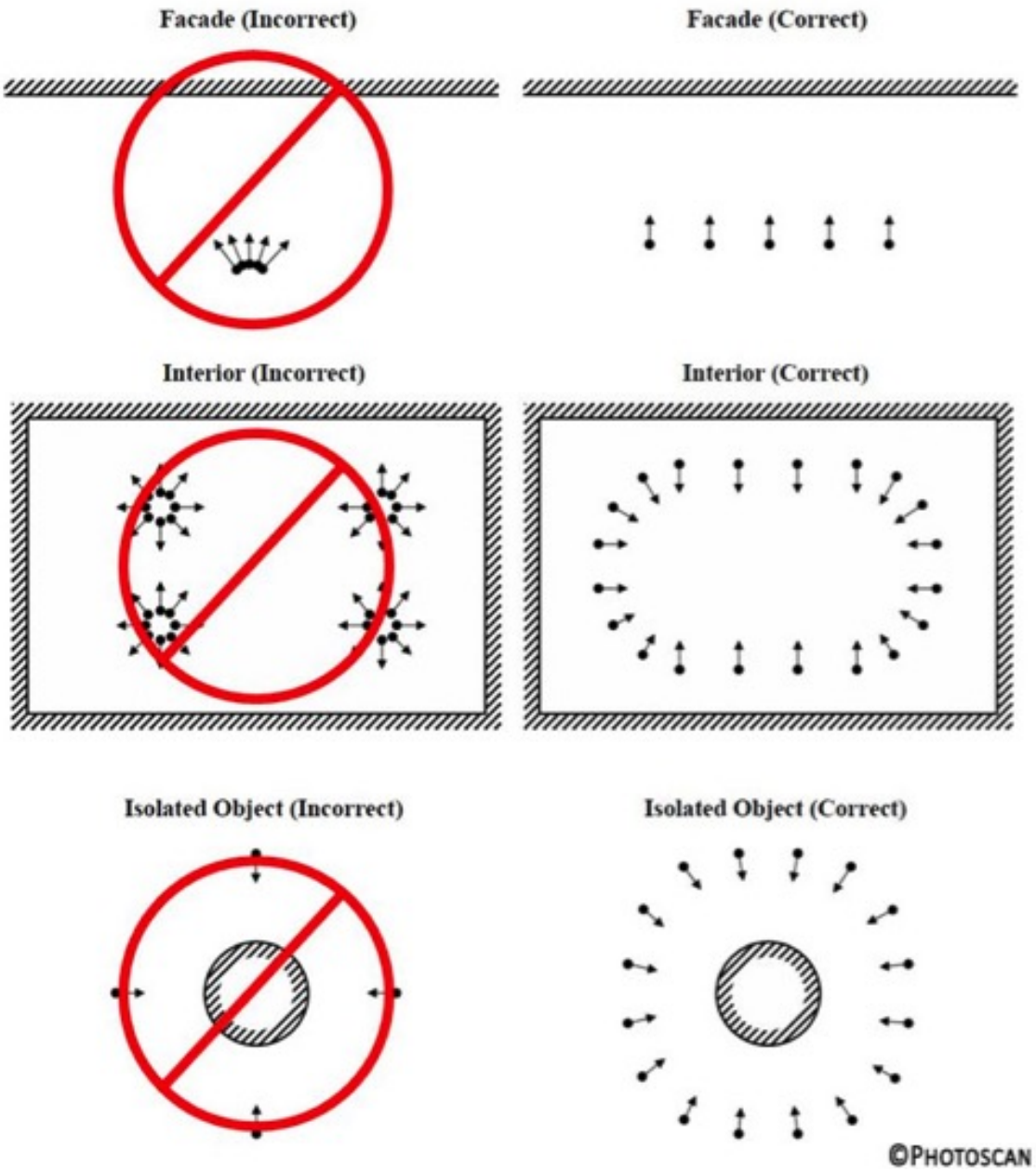

Figure 2.1: Guide for Proper Image Capture with Photogrammetry: Top Left: Incorrect way to capture objects in a line, Top Right: Correct way to capture objects in a line (i.e. stream), Middle Left: Incorrect way to capture objects of interior, Middle Right: Correct way for objects interior (i.e box), Bottom Left: Incorrect way for capture for objects in isolation, Bottom Right: Correct capture for objects of isolation (i.e. soil pyramid) (Agisoft.com).

Figure 2.2: Proper coded target placement is crucial, the green check mark represents proper coded target set up. The target must not be altered because Agisoft will not recognize it, the target must be flat and resemble a circle consisting of black and white segments (Agisoft.com).

accuracy of the models the volume measured with Agisoft Photoscan was compared to that of the known volume calculated analytically. Models were considered accurate if the normalized error between the known and measured models was less than 5%. The box and pyramids had a known value calculated with basic geometry, (Equation 2.1a and 2.1b).

$$V = l * w * h \tag{2.1a}$$

$$V = \frac{1}{3}(a^2 + ab + b^2)h \tag{2.1b}$$

The same workflow process in Agisoft Photoscan for pre-processing models was used for each study, keeping the default settings as recommended from Agisoft Photoscan at each step. The following processes were selected for pre-processing of photosets: align images, optimize alignment, build dense point cloud, build mesh, build texture, and detect targets. Additional steps such as input of control points and creating scale-bars for measurement were conducted after models were produced. The steps in the workflow process allow models to be constructed.

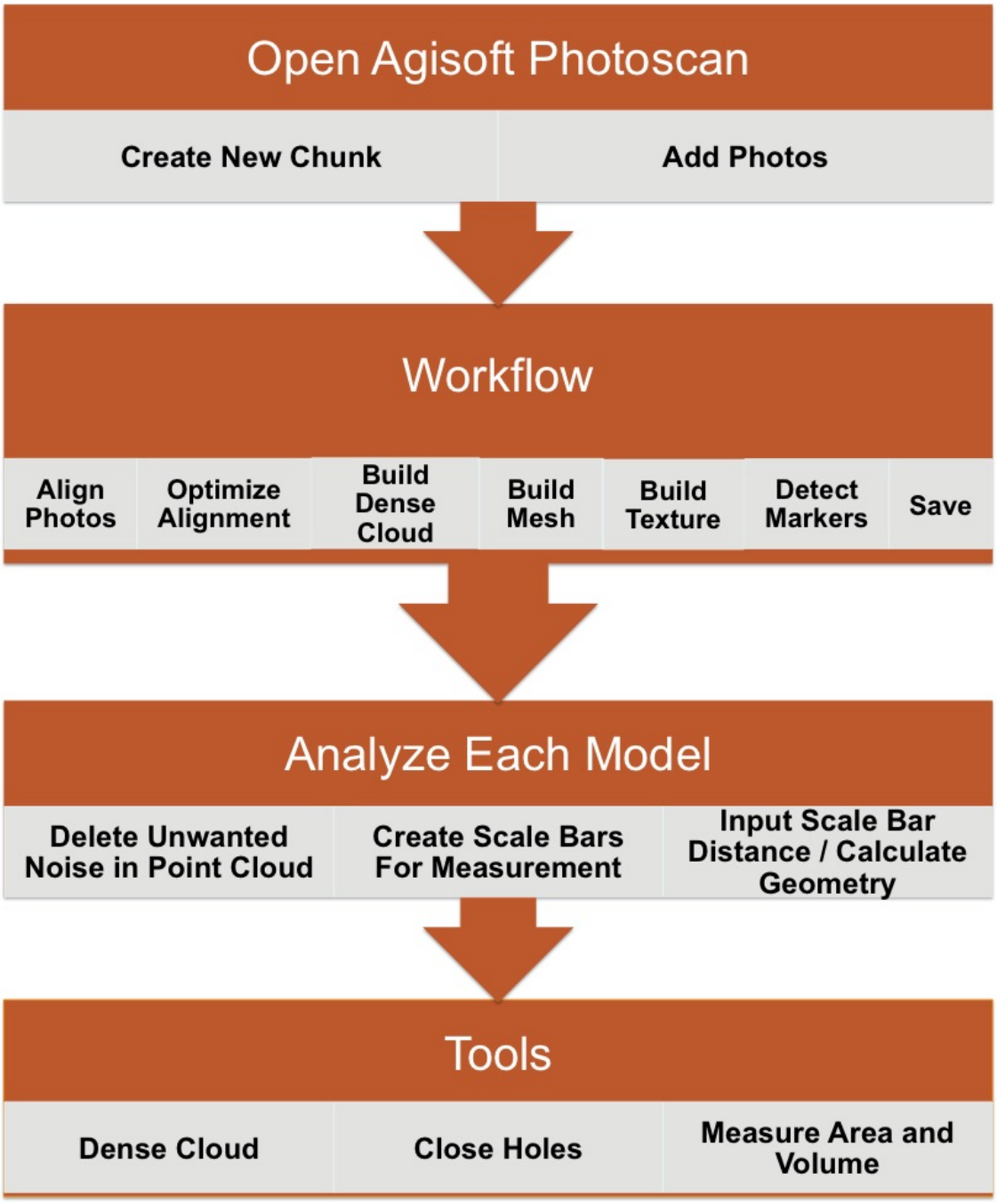

Figure 2.3: Basic processing steps used in 3D model construction through Agisoft Photoscan. The first two processes are data input into Agisoft. A chunk is a multitude of photos from a single survey used for 3D reconstruction..

2.3.1 Camera Comparison

Two cameras were used for this study: a Nikon D90 digital camera (DSLR), and a Samsung Galaxy S4 cell phone (Table 2.1). The cameras were selected based on cost and accessibility. Most people have access to a cell phone with a camera built in rather than purchasing a separate more expensive DSLR camera. The DSLR and cell phone camera have different image quality and types. The DSLR takes high quality RAW images. RAW images are typically 24 or 48 bit images that are minimally processed and stored as taken. The Samsung takes high quality JPEG images, which is a major compression of a photo. During this study, images were used as data for creating models; therefore, RAW images from the DSLR were converted into TIFF 8 bit images for input into Agisoft Photoscan. However, JPEG images from the cell phone were not converted into TIFFs due to the existing compression. When a RAW image is converted into a TIFF file information is not lost; however, file information is lost with the compression of a JPEG image. RAW Therapy software program was used to convert all RAW images from the DSLR to TIFF files. The automatic capture setting was used throughout the study. The automatic setting allows the camera to recognize light for a well balanced exposure and non-blurry image. This setting also sets the aperture and shutter speed automatically to ensure all images captured are of the same quality.

Table 2.1: Camera Comparison for the Selected Camera Technologies.

Camera	**Image Type**	**Auto Focus**	**Camera Resolution**	**Focal Length**	**Optical Zoom**
Nikon D90	RAW	Yes	12.3Mp	16-35mm	No
Samsung Galaxy S4	JPG	Yes	13Mp	31mm	No

2.3.2 Box Study

A cardboard box (29.0 cm x16.5 cm x 23.0 cm) was analyzed with photogrammetry using a Nikon D90 DSLR and a Samsung Galaxy S4. The images taken were at a fixed focal length (no zoom) for both cameras. Image capture with the phone was taken 0.9 m away from the box and the DSLR images were taken 1.5 m away due to the field of view of the cameras (Figure 2.7). The data was processed through Agisoft Photoscan with the batch process.

A calibration test was run to determine the amount of images needed to create an accurate model of the box. Twenty-four images were the lowest number of images needed for accurate model reconstruction. For the first test, coded targets were set up around the box (Figure 2.2), to act as control points recognized by the software. Each target was marker type of 12 bit, with a center point radius of 10 mm recommended by Agisoft Photoscan. A minimum of six targets were placed around the box to ensure each image had at least one marker in the image for reference point, and a maximum of seven targets were used. Images were then taken from different angles. Overlap of 60% side overlap and 80% of forward overlap is recommended. The box study had a set minimum of six images to achieve proper image overlap, with a maximum of twenty-four images to be studied.

A chunk was created with each new model. A chunk is also known as a photoset that is selected for each model. In the batch process several different parameters were entered for the program to run. The parameters include align images, optimize alignment, build mesh, build dense cloud and build texture and detect markers. Once this process was completed a 3D model was produced. In some cases, the software did not recognize the coded targets, therefore manual manipulation to place the targets was required. These markers can be saved and then imported into models without target recognition.

Once coded targets were set around the box, scale bars could then be created using the distance between two targets. Each scale bar was measured by using the corresponding two coded targets with a ruler. The scale bars standard error of distance is known for a more

accurate model automated through Agisoft Photoscan. The scale bar is then recognized in Agisoft Photoscan to measure distance between points and determine volume while creating an accurate geometry of an object.

After the set up of scale bars, unwanted noise of the model is deleted. The selection tool was used to select the part of the model used for volume calculation. The close holes tool was used to fill in the gaps that may be within a model. Once processed, volume and area were calculated by using the build mesh menu button.

The initial test was evaluated with no vegetation. Trials conducted for this study include models run with 15 to 23 images and replication of 20 models per trial. The first six images were included in every trial to create the designed 60% side overlap within photo models. To generate the remaining images per trial, R studio was used to create a random pool. The remaining images per set were labeled. The R script used was sample.int (48,1). This code generated the remaining photos to complete each set of images. The same script was used to determine the quadrant in which vegetation was placed. Once random photosets were compiled, chunks in Agisoft Photoscan were created for the various photo sets. Chunks contained separate image sets that were based on the number of image numbers it contained for each chunk.

2.4 Evaluation of Leaf Area Index

Artificial vegetation (English ivy) was used in three treatments to evaluate increasing leaf area index with each treatment. Studies include Vegetation 1, Vegetation 2, and Random vegetation test (Table 2.2). Vegetation was added in increments onto a styrofoam board in front of the cardboard box.

Table 2.2: Evaluation of Each Box Study with Corresponding LAI.

Treatment	**LAI**	**Images**
Vegetation 1	0.07	24
Vegetation 2	0.105	24
Random	0.129	24

Leaf area index was estimated using the graph paper method as described by Yan et al. (2016) and Pandey and Singh (2011). Artificial vegetation was placed around the box to determine the impact of vegetation on photogrammetric models. Yan et al. (2016); Pandey and Singh (2011), and Ross (1981) recommended that the area of a leaf should be determined by drawing a leaf's outline on graph paper and measuring the enclosed area. Once the surface area of the leaf was calculated it was divided by the area of the underlying styrofoam board. Vegetation was then tested at various height and density intervals. Vegetation was added in three stages, (i) Vegetation 1: eight stems at 15.2 cm height added 21 cm away from the box on each face and corner of the box (Figure 2.4), (ii) Vegetation 2: four stems at 15.2 cm then added to each side of the box, attached directly to the box surface (Figure 2.5), (iii) two stems at 30.5 cm were added randomly in quadrants, then followed by increments of one stem per trial. Each stem of English ivy had an LAI of 0.009 for Vegetation 1 and 2 and an LAI of 0.012 for the random test. Twelve quadrants (16cm by 20cm each) were set on each side (4 sides) of the box for a total of 48 quadrants (Figure 2.6). LAI was determined by dividing the surface area per stem by the total surface area of the underlying styrofoam board. The total area of the board was 15,360 cm^2. Each stem evaluated for Vegetation 1 and 2 had an average surface area of 134.64 cm^2, and each stem added to the random study had an average surface area of 186.84 cm^2. LAI ranged from zero as a control to the highest LAI of 0.48.

Figure 2.4: Vegetation 1: Vegetation was added by using English ivy, eight stems were placed around the box on a styrofoam board.

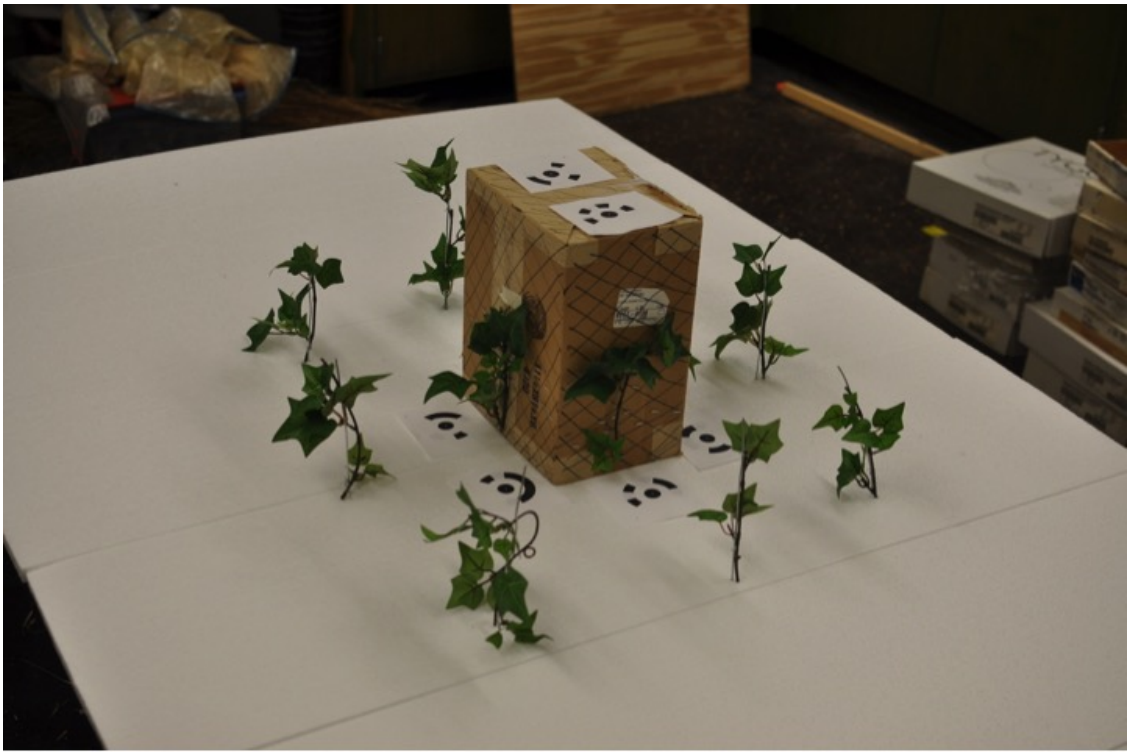

Figure 2.5: Vegetation 2: Addition of four stems of English ivy for a total of twelve stems placed around the box.

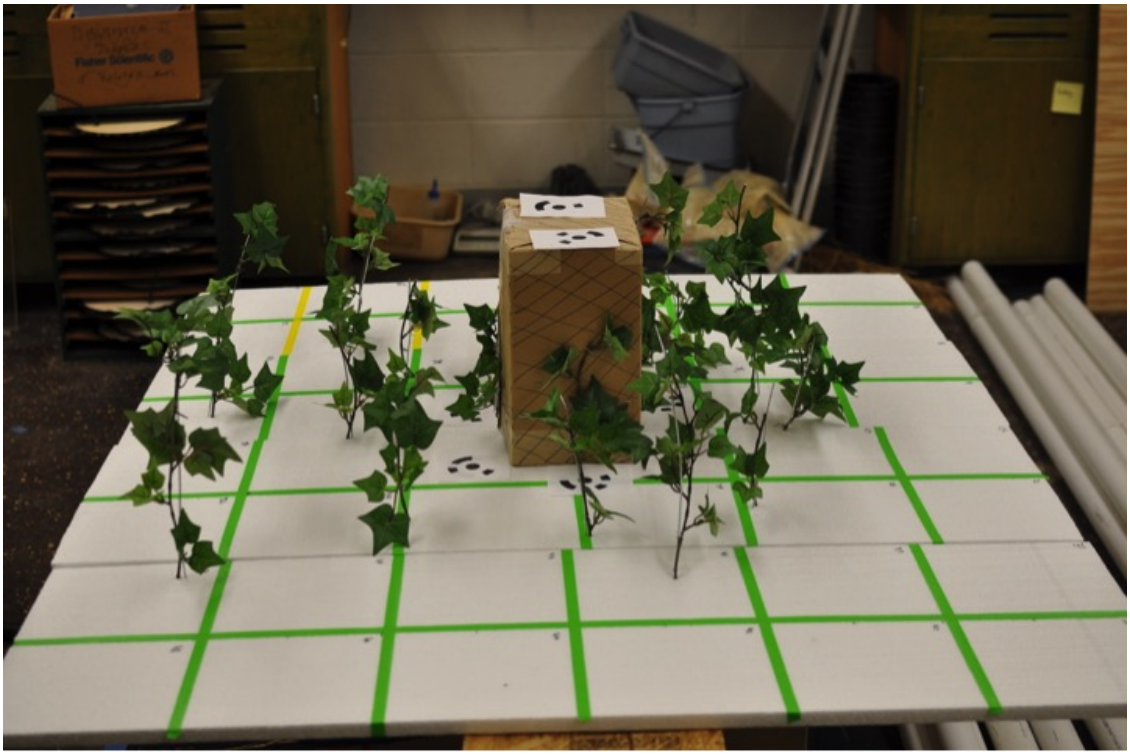

Figure 2.6: The random vegetation study added English ivy in separated quadrants at random. Random placement generation was created through R, a statistical and analysis software

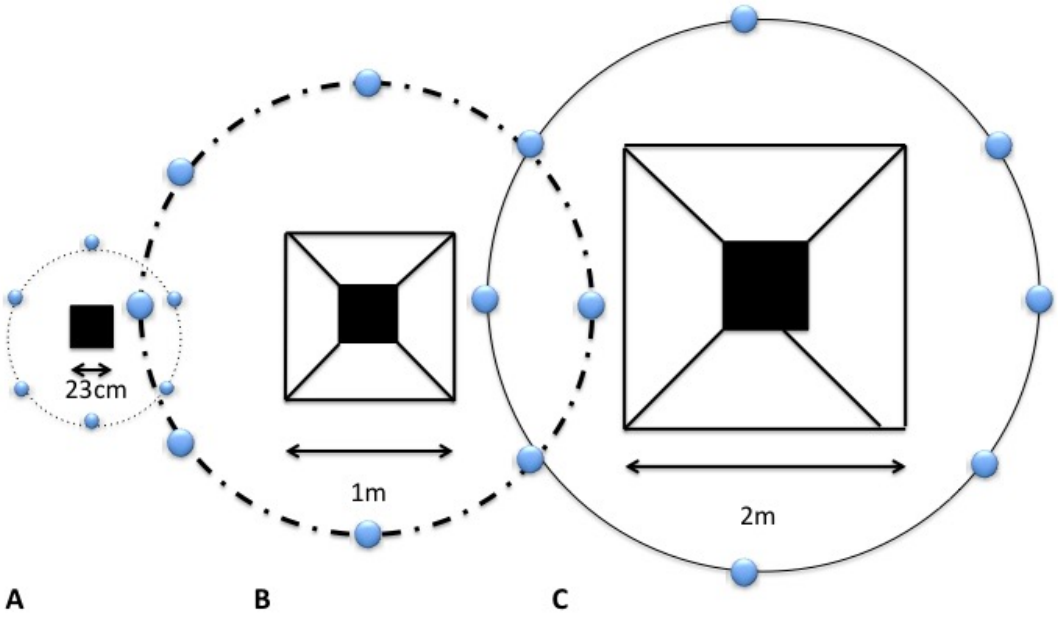

Figure 2.7: Image capture for controlled studies discussed in each section. A. Box study image capture, B. Small pyramid study image capture C. Large pyramid image capture. Each small dot represents camera positions, between each of these positions an additional three images are captured.

2.5 Vegetation Obscurity Index

A secondary method, vegetation obscurity index (i), was used to determine vegetation effect on a models accuracy. To determine the vegetation obscurity four images were selected from each box study. These images corresponded to each side of the box (Figure 2.8). Selected images were imported into Inkscape, an image processing software. In Inkscape each of the four images were overlaid with a grid and the grid was used as a measuring tool for vegetation obscurity. The images were then exported and labeled as north, south, east, and west in separate folders with the name of each study (Figure 2.9). To evaluate vegetation obscurity the number of grid spaces covering the face of the box were counted. Vegetation obscurity was equal to the number of grid spaces containing vegetation divided

by the amount of total grid spaces on the corresponding face of the box. This method works well when evaluating vegetation in a side view, or in cases when LAI technology could not be assessed. By using vegetation obscurity in this study more accurate data can be derived from the measurement. The reason is that the vegetation being measured is compared to the box and not the styrofoam board for which LAI accounts. LAI accounts for the area covered per one leaf or collection of leaves in a plain view or from top down. Vegetation obscurity index accounts for the area of leaves covering a surface from a side view. Both methods account for obscurity of a surface from vegetation.

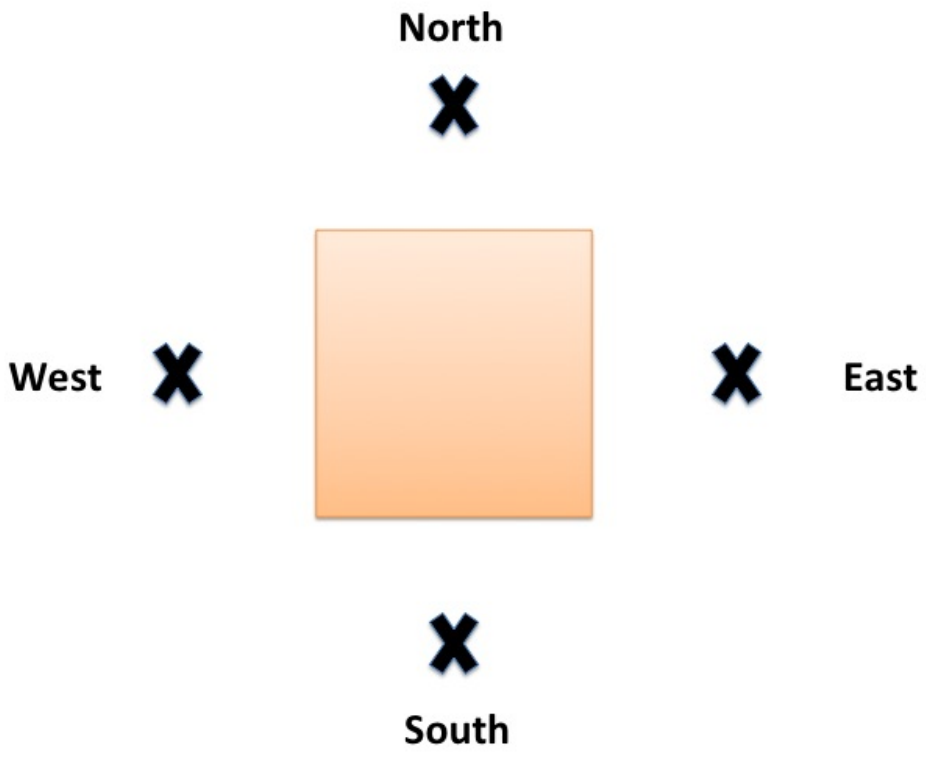

Figure 2.8: Images selected to calculate vegetation obscurity, each image is labeled by its location around the box

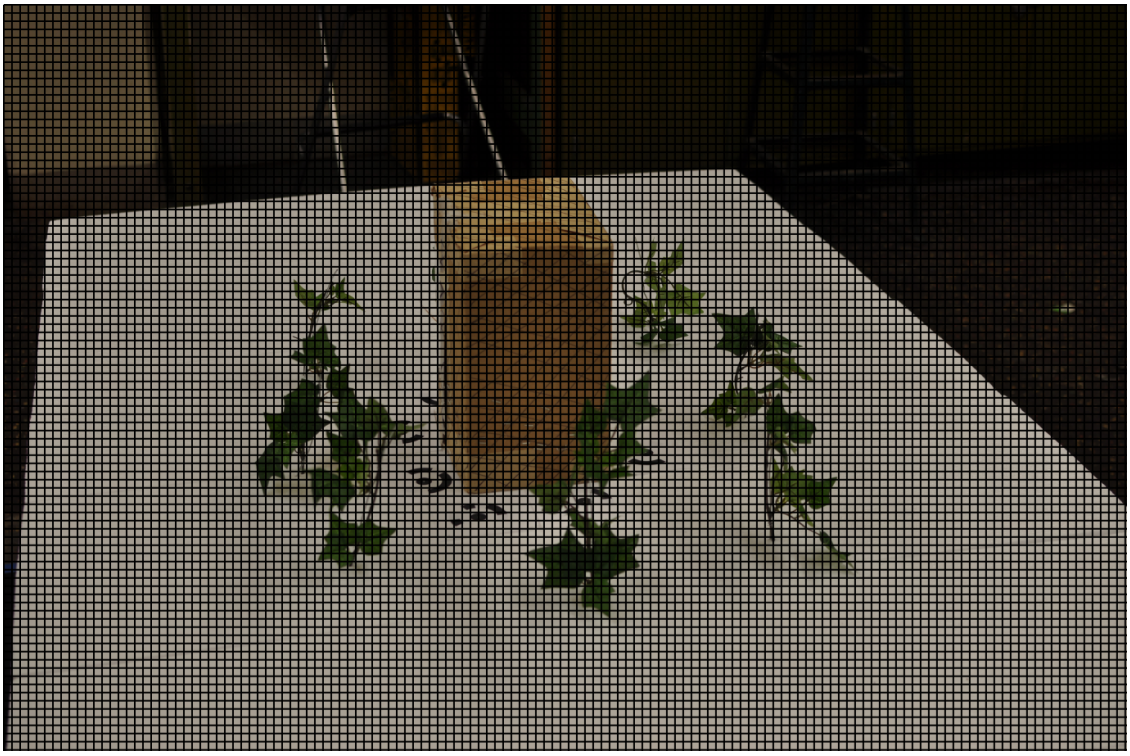

Figure 2.9: South facing image of the box with a grid overlay for vegetation obscurity index. The same grid was used for vegetation obscurity evaluation for the pyramid study

2.6 Soil Pyramids

Two soil pyramids were constructed at the Auburn University Turf Research Unit in Auburn, Alabama. Soil from the field location was shaped into truncated pyramids (Figure 2.10). The soil is described as Pacolet sandy loam, with 6 to 10% slopes. The pyramids sizes were 1m x 1m and 2m x 2m at the base and the tops were 30.5 cm and 61.0 cm, respectively. German foxtail millet was selected as temporary vegetative cover and broadcasted on each pyramid at a seeding rate of $2g/m^2$(Figure 2.11). The small pyramid had a total surface area of $2.43m^2$ and large pyramid a total of $8.86m^2$. Trials were separated by size for image capture and pre-processing. Forty images for the small and large pyramid, were captured and used for pre-processing in Agisoft Photoscan. Image capture distance refers to the distance from the object to be captured to the camera location. Image capture distance for the small pyramid was at 1.5m for the cell phone and 1.83m for the DSLR. The large pyramid image

capture was at 2.75m for the cell phone and 3m for the DSLR. This distance allows for a full capture of the pyramids for each camera type (Figure 2.7).

Agisoft Photoscan coded targets were placed around the pyramids before images were captured. Eight coded targets were used for the small pyramid and 10 were used for the large pyramid. To determine the number of targets needed to accurately predict volume, a test trial of images was taken to ensure at least three targets were visible in every image. Coded targets were spaced evenly with at least one target per side or corner of the scene to be captured. The coded targets are recognized by Agisoft Photoscan once images are input into the program. The coded target size recommended by the software is marker type: 12 bit, with a center point radius of 10mm, and 6 targets per page.

Markers were measured for distance between each marker to set up a scale bar. The markers were laminated and placed on the ground with a long nail in the middle to secure them to the ground and location. Images were then captured for pre-processing. After image capture the images were processed through Agisoft Photoscan. Processing was done as follows; 1) input images into Agisoft Photoscan as chunks, 2) use batch process to create 3D models, 3) create scale bar from field measurements, and 4) analyze 3D models for volume. Pyramids were evaluated over five weeks to analyze the effect of vegetation growth on volume accuracy. Table 2.5 shows the relationship of vegetation growth to each image set (week 0 - week 5). Week zero had bare soil at 0% vegetative coverage and week 4 had 100% vegetative coverage.

Percent vegetation coverage was evaluated every survey based on ratio of grass to soil visible on each of the pyramids (i.e., 1/4 covered is 25%). This technique was used throughout the surveys which is five total weeks of growth at 100% and no visible soil. The vegetation obscurity index was used for the pyramid study as it was for the box study. A grid containing 100 squares was imposed over an image of the pyramid from each week. The number of squares containing vegetation represented the precent soil or pyramid covered.

Figure 2.10: Large pyramid after construction at week zero, bare soil and no vegetation obscurity. Coded targets were used to increase model accuracy.

Figure 2.11: Large pyramid at week 5, 100% vegetation coverage. Coded targets were used to increase model accuracy.

2.7 Stream Studies

The stream study was conducted along a reach of Parkerson Mill Creek in Auburn, Alabama (N32.577342, W85.503990) as it flows behind the Auburn University Turf Unit. A camera tripod was used to capture images at a constant height and angle. The camera tripod used for image capture was set at 1.5 m in height for all surveys of the stream site. Image capture used for this study is called linear image capture (Figure 1.4). The stream was restored in Spring 2015, and SFM surveys were conducted every two weeks for seven months. Two individual studies were conducted to evaluate stream change over time . The initial study evaluated two survey methods, the traditional total station method and SFM method. The second study evaluated DEMs from each SFM study to the baseline transect comparison.

2.7.1 Total Station Data

Total station data were collected by the City of Auburn, Water Resources staff on April 20, 2016. Total station data are considered reference data for the photogrammetry surveys. Only one total station survey was conducted for this study. Seven transects were surveyed for the study site. To compare photogrammetric surveys to reference data only the transect coordinates of the stream bank surveyed with photogrammetry were analyzed for accuracy. Total station data were collected using two control points set at each end of the project with a Spectra Precision RTK GPS. The RTK fix was provided by the ALDOT CORS station ALA1 in Auburn, Alabama. After the control points were set, a Nikon NPL-322+ total station and a rod with a standard prism was used to collect the geometry data. The total station was set up over the southernmost control point, and the backsight was made to the northernmost control point. This placed all subsequent shots in the Alabama State Plane East coordinate system on the NAD83(2011) datum. Topographic data were collected along cross-sections of the project reach. Significant geomorphic features (i.e. top of bank, toe of slope, edge of water, thalweg, and other topographic breaks) were collected to create surface model of the project area.

2.7.2 Photogrammetry Data

Images were captured biweekly using the DSLR and cell phone camera for a total of 24 SFM surveys. The images were captured using a camera tripod at a height of 1.5m at a 0.5m distance. The camera positions were located within the creek approximately three meters away from the stream bank to be surveyed. At each camera position five images were taken, one straight forward, two at both 90 degree left and right, and two at 40 degrees right and left of center. Image capture was repeated over time for a one year period following restoration efforts. Photogrammetric surveys were collected using the following steps:

1. Install ground control points and capture GPS points for each target.

2. Facade image capture.

3. Capture image sets with cell phone and DSLR cameras.

4. Pre-processing using Agisoft.

Nineteen ground control points (GCPs) were installed using coded targets from Agisoft Photoscan. These points were collected with a Trimble GeoXH GNSS and each point was calculated for a minimum of 300 points. GCPs increase the accuracy of a model by connecting the images to a location. It is recommended that at least three GCPs are in a SFM survey; however, multiple GCPs create a more robust survey (James and Robson, 2012). The models were produced in the WGS84 geographic coordinate system and the UTM16N projected coordinate system in Agisoft Photoscan. GCPs allow a better dense cloud creation, which creates a more precisely located model. Each target was laminated for weatherproofing, stapled to survey stakes and 1m rebar was installed at each point. Once points were installed, a linear image capture was used, a linear image capture is a simple image capture along a line. Images were taken every half meter with multiple directions (i.e. full field of view). Half meter camera positions were selected based on previous studies recommending that more camera positions lead to more overlap among images (Dietrich, 2016). Also, it is important that at least three targets are within each image to assist in stitching of images together during pre-processing. Time of day also impacts model accuracy. Surveys were conducted at noon when sunlight was evenly dispersed over the stream.

2.8 Transect Survey and Photogrammetry Comparison

An initial assessment comparing one SFM survey to the transect survey was established to set a base line for the remaining surveys. To evaluate survey techniques total station cross section data and photogrammetry output raster from the first survey (survey 1) were compared. Transect surveys are made up of GPS points along a line, and photogrammetry surveys are high resolution point clouds, models and DEMs (Figure 2.13). The DEMs created

Figure 2.12: Linear Image capture was used to collect the images used in Agisoft Photoscan. The figure shows each camera station and GCP used throughout the stream study.

from post survey 1 were compared to the transect data for an initial assessment evaluating survey methods. An R script was set up as a loop to run data the same way for each DEM. The DEMs were created from post survey 1. To produce DEMs the following steps were taken in Agisoft: 1. build DEM, 2. export DEM to :WGS84 UTM 16N, 3. save DEM as TIFF file with specific survey name (i.e. Ps1dslr, Ps1Phone). Once created each DEM was saved in a raster format. Using the transect survey as a line shape file and the DEM raster files, a comparison of survey methods was evaluated using an R code (Appendix A.0.1). The normalized root mean square error (NRMSE) calculated shows how much error there is between the photogrammetric surveys and the total station survey. Survey 1 was conducted exactly one month after the final Total station survey. This comparison will be used as a baseline for the remaining models conducted with SFM.

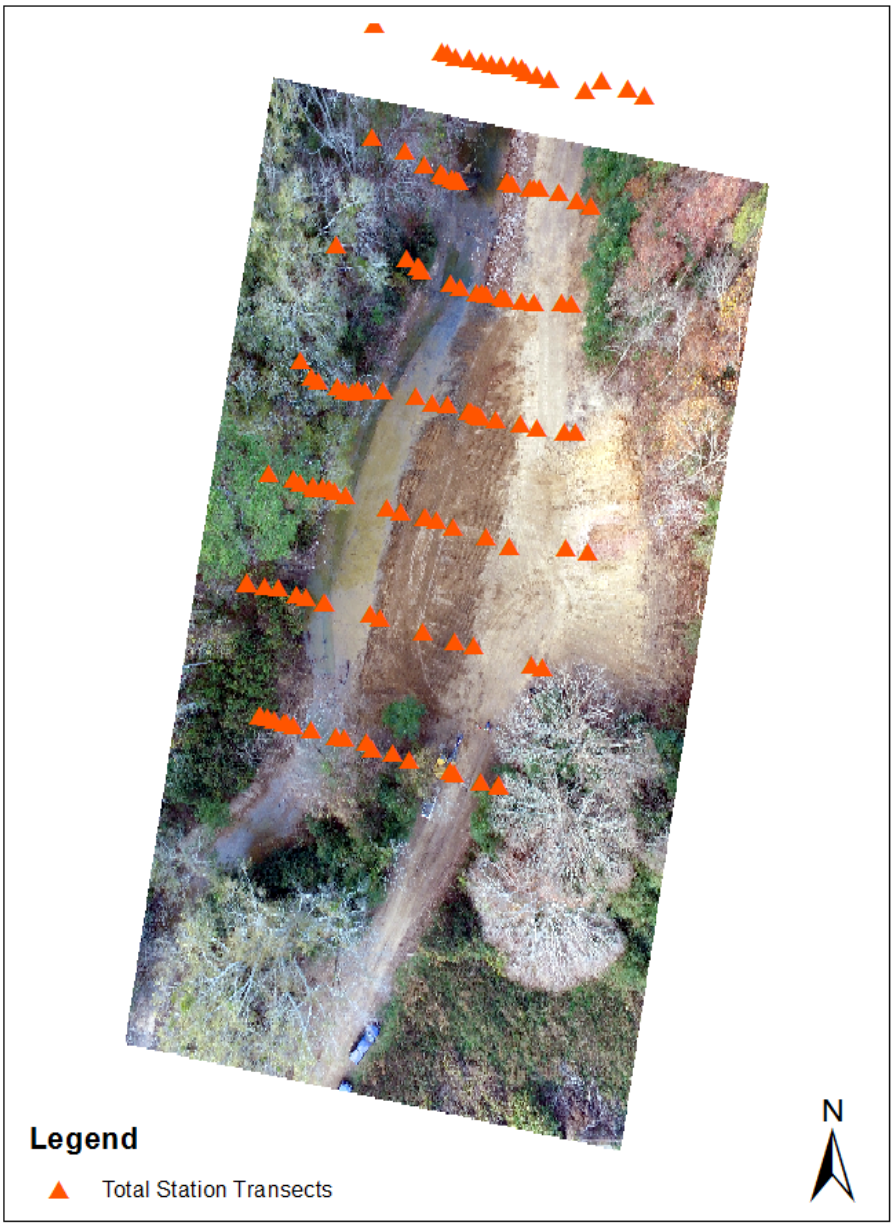

Figure 2.13: Schematic showing a transect survey from the total station survey and imagery depicting the extent of a photogrammetry survey.

2.8.1 R script

Using the statistical analysis program R studio (RStudio Team, 2015) a script was developed to evaluate data of the digital elevation models produced from Agisoft Photoscan; the steps for this script are listed in Appendix A.0.1. Transect survey lines were overlaid on the DEM's created from survey 1. R was then used to compare a DEM (raster file) to the transect data (GPS, shape file). The NRMSE was used to calculate the difference between the elevations of points along the transect data. When the script was processed, the DEM points that correspond to the transect points were compared.

A secondary R script was used to evaluate the second stream study, evaluation of DEM change over time (Appendix A.0.2). This analysis evaluates the DEMs as they change over time , comparing each DEM to the first DEM from survey one. This study was used as a baseline study as well as comparing each DEM to the last survey to better understand stream change over time. Stream change over time can be noted through the elevation changes among DEM points.

2.9 Statistical Analysis / Root Mean Square Error and Standard Error Maps

Once models were run and analyzed a simple root mean square error (RMSE) was calculated. A root mean square error analysis predicts the average y value associated with a given x value. First we must obtain the spread of the y values around the average. The RMSE is frequently used to measure the difference between the values predicted and the values actually observed in a model. The RMSE values can be used to distinguish a model performance in a calibration period versus validation period as well comparing individual model performance to that of other predictive models (T and Draxler, 2014; Holmes, 2000).

The normalized RMSE (NRMSE) was used to compare observed data to reference data. To calculate elevation difference (total station point and SFM point) the normalized root mean square error of linear regressions between total station GPS points and SFM elevations were evaluated with the following equation (Taylor, 1997).

$$S.E. = \frac{standard - deviation}{\sqrt{n}} \tag{2.2}$$

$$NRMSE = \frac{\sqrt{\frac{1}{n}\sum_{i=1}^{n}(V_{estimated} - V_{known})^2}}{V_{known}} \tag{2.3}$$

From equation 2.2, n is the number of observations, $V_{estimated}$ is the observed values or the elevations calculated with Agisoft Photoscan, and V_{known} is the calculated or reference value elevation of the total station survey. The normalized RMSE was also used to compare DEMs over time. A boundary was created for the DEMs to ensure all DEMs were of the same extent, once created the DEMs raster points were analyzed by comparing corresponding raster points. These raster points or spatial points are also elevations within the DEMs. To understand change over time the DEMs were compared to the first studies DEM and the last surveys DEM.

To evaluate error among models and compare camera technologies standard error maps were created. Standard error (S.E.) equation 2.3, is a measure of spread between values, which is a measurement of accuracy between sampled means, such as comparing raster points to a known point. Standard error maps will show error among raster points between each DEM, thus showing the spread (error) of the values over time when comparing DEMs. The standard error shows the differences in DEMs from survey 1 and survey 12 which is the actual points of comparison. Standard error maps were created to show the accuracy of the cameras as well as gaps in the DEMs which lead to increased error in the overall models performance.

2.10 Comparing DEMs Over Time Through Evaluation of Baseline Study Data

Using the base line data from study 1 (comparison of post survey 1 to transect data) DEMs were evaluated for change over time. Models were compared by analyzing corresponding raster points among the DEMs created from survey 1 and survey 12. Two different DEMs

were created: an interpolated dense cloud (highest accuracy) and a non-interpolated mesh (lowest accuracy). Photoscan will generate a DEM on the specified resolution, build DEMs from the dense points directly with an "Inverse Distance Weighting" (IDW) interpolation. This allows a more dense DEM, with higher quality and resolution. On the other hand a DEM from a mesh cloud is interpolated as a Triangulated Irregular Network (TIN) where Agisoft linearly interpolates the dense points as small triangles, with a lower resolution and lower density. Both methods of creating DEMs are good ways for interpolation, however, for surveying purposes a DEM from a dense cloud would be of higher quality. The interpolated dense cloud method generates less noise within models and less obscurities. Each of the methods for creating DEMs were necessary to create a complete DEM for measurement and evaluation.

All DEMs were clipped to a polygon to ensure all models were of the same extent. DEMs were then input into an R code where a template was created from the models common raster points. Raster points were assigned with the number "1" for points in surveys that were aligned and "NA's" for points that were not aligned. Alignment of raster points meant that each DEM created had a corresponding raster point to compare to. To create a DEM template a boundary was drawn around the study area through ArcGIS. This template was used to compare DEM raster points over time from survey 1 and survey 12. Change over time between DEMs can be an indication of stream change such as erosion or deposition. When DEMs were compared to the first model the error should increase and when compared to the last model the error should decrease. Increase or decrease in RMSE among DEMs will show changes along the study area.

Chapter 3

Results

Results of the study show the capabilities and constraints of using photogrammetry as an alternative method of surveying and reconstructing objects at various scale. For each study conducted, images were analyzed through Agisoft Photoscan and results for three separate scale objects. The results built off individual studies and focus on factors which affected photogrammetry. The results indicate that control points must be established, and that vegetation has adverse effects on the accuracy of models. Models were used as a verification of the capabilities and constraints of photogrammetry. Likewise, photogrammetry capabilities shown in the results verified the potential uses at various scales for 3D model reconstruction and measurements.

3.1 Box Studies

The purpose of the box study was to gain information in a controlled setting of the capabilities and constraints of SFM photogrammetry. The box study evaluated vegetation effects and number of images required for producing models with low error. An accurate model for the following studies had less than 5% error in volume from the known measurement of the box. The known volume was measured at 0.0108m^3. However, this study also analyzed a threshold of error based on number of images used in a model. The threshold of images proves to be a better measurement of accuracy for these models. Based on the results, 5% error seems to be limiting when evaluating the capabilities of small scale SFM photogrammetry. Models may have greater than 5% error and still produce quality models. The box study required 19 images for an accurate model. The lowest model error was achieved between 19 and 24 photos, but at 21 photos error was greater than 5% (Figure 3.1).

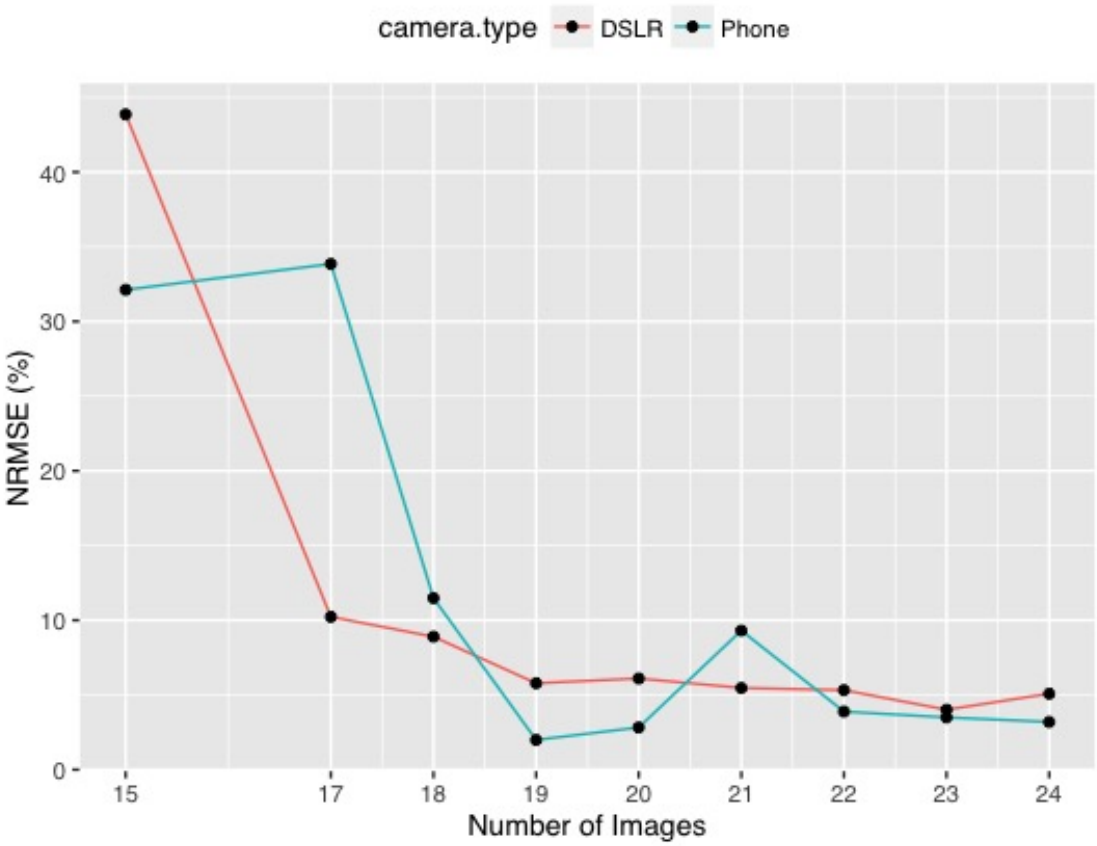

Figure 3.1: Box Model Error: NRMSE compared to number of images. The plot indicates that with less than 18 images both camera technologies are unable to produce measurable models. With 24 images the models were at or below 5% error.

Results indicate that with less than 18 images models had very high error and indicated that models accuracy diminished once this threshold was met.

3.1.1 Vegetation 1, Vegetation 2 and Random Vegetation Box Study

The goal of this study was to determine how LAI and vegetation obscurity index (i) affect models accuracy. Using various amounts of images ranging from 19 to 24, models were analyzed for volume estimation. The following studies show a correlation between increased LAI, obscurity index and decreased models accuracy. Models for the following studies had greater error when fewer photos were used to create models.

For the first vegetation study (Vegetation 1), vegetation obscured a model at twenty-four images, and the LAI for this study was 0.07, and obscurity index was 7%. Results show that as vegetation was added to a model it becomes inaccurate. A comparison of the cell phone to DSLR camera showed that each technology produced models for volume estimation in Agisoft. Results indicate that models created using the DLSR were not accurate with less than 20 images. The models produced with the cell phone were inaccurate with less than 24 images (Figure 3.2).

For the second vegetation study (Vegetation 2) the LAI was increased by adding four additional English ivy stems directly to the box. The goal of the study was to evaluate error in models as vegetation increases. Results show that both cameras were able to reproduce and measure a volume of the box even with increased vegetation. Both camera types had a varying degrees of accuracy among the photosets. The LAI for this study was 0.105 and the obscurity index was 19%. The figure indicates that model accuracy varies among image sets and that models were not accurate and there was no correlation to the number of images (Figure 3.3). As results also indicate that accuracy varied among photosets, Agisoft interprets photosets differently and independently, therefore, error in models can vary based on number of photos. Accuracy among models was also affected by those photos that were randomly drawn for reconstruction.

The last vegetation study focused on an LAI greater than 0.129 and obscurity index greater than 29%. The Random vegetation study required a quadrant system (refer to section 2.0.2, Leaf Area Index). Vegetation was added to randomized quadrants produced in

R studio. LAI and vegetation obscurity increases as vegetation was added to the random quadrants. Based on the previous vegetation studies, a minimum of twenty-four images were selected and modeled. Results show the NRMSE increases when both LAI and vegetation obscurity increases (Figure 3.4, 3.5). Models that were unable to be evaluated were blank and given an NA, meaning the placement of the stem or the corresponding LAI prevented construction of that model. Accuracy varied in this study, and results indicated that vegetation obstructs the accuracy of models. This study suggest that with an LAI greater than 0.1 models become less accurate independent of image sets.

In summary, accuracy of models decreases when 0.07 LAI is added to the box and at 0.035 models are no longer accurate and photosets accuracy becomes independent of error. Results also indicated that with less than 21 images, models accuracy decreases. Examples of high quality and low quality models from the box studies are shown in Figure 3.6.

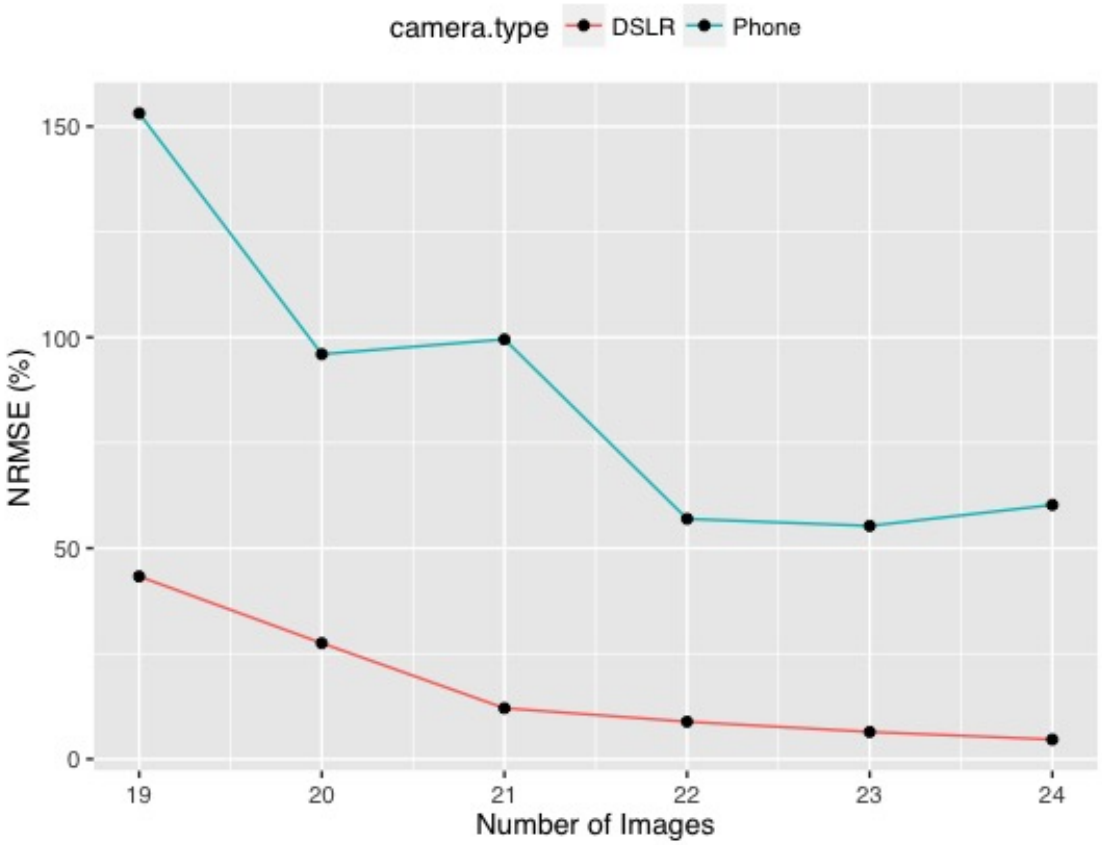

Figure 3.2: Vegetation 1 Model Error: NRMSE created when vegetation is added at 0.07 LAI and 7% vegetation obscurity, with respect to number of images.

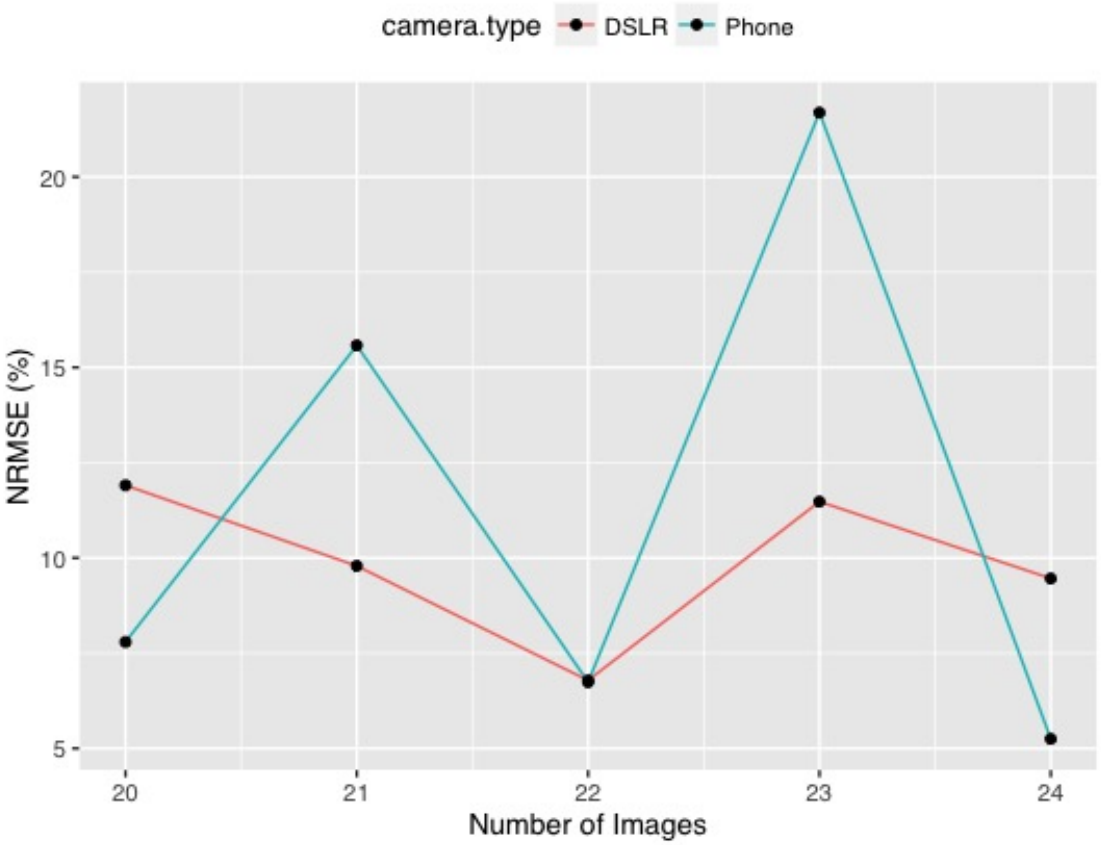

Figure 3.3: Vegetation 2 Model Error: NRMSE created with an LAI of 0.105 and vegetation obscurity of 19%, based on decreasing number of images. Error is independent of number of photos.

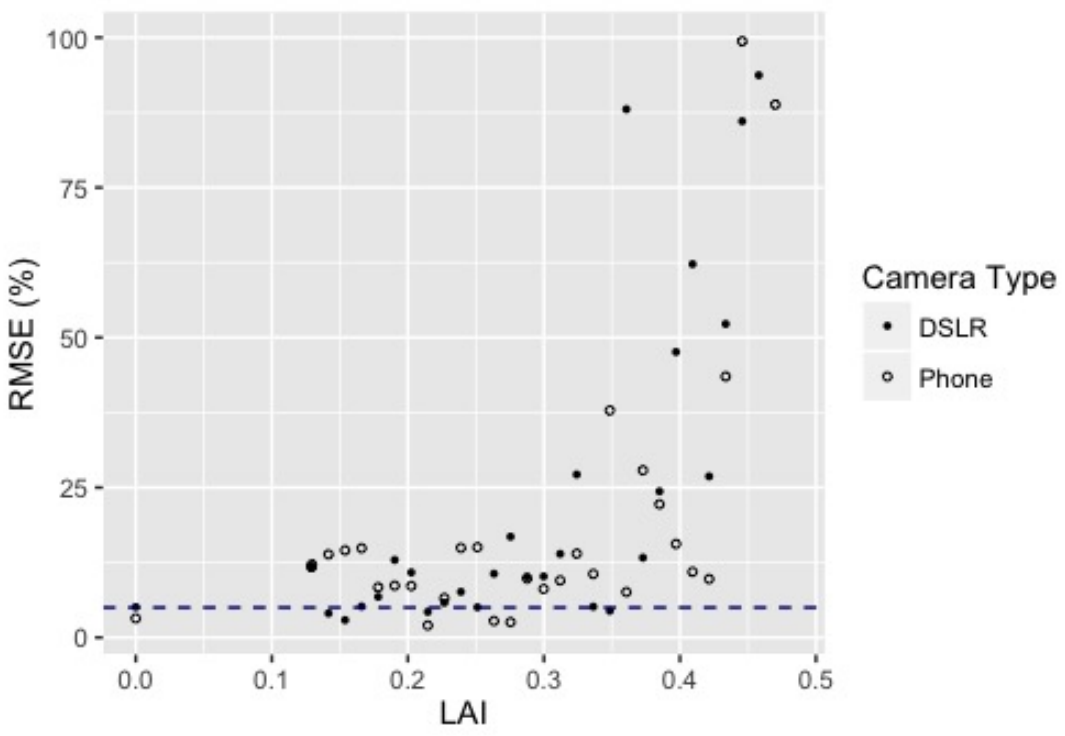

Figure 3.4: Random Box Model Error: NRMSE in a model based on increasing LAI for 24 images. There were 2 Missing trials for which Agisoft could not create a meaningful model. NRMSE sharply increases at LAI 0.35, suggesting that accuracy declines at this point. The dashed line represents 5% error.

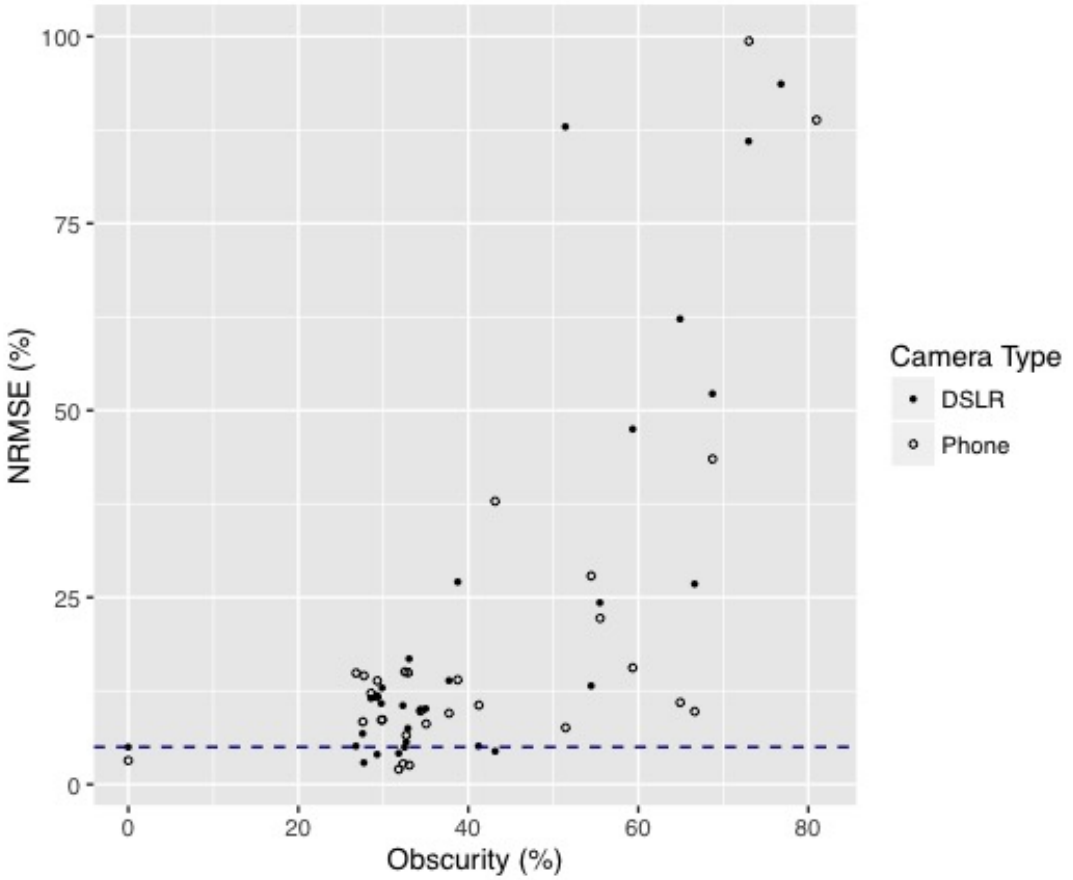

Figure 3.5: Random Box Model Error: NRMSE in a model based on increasing vegetation obscurity for 24 images. There were 2 Missing trials for which Agisoft could not create a meaningful model. With a vegetation obscurity of 50% NRMSE is greatly increased, suggesting that accuracy declines at this point. The dashed line represents 5% error.

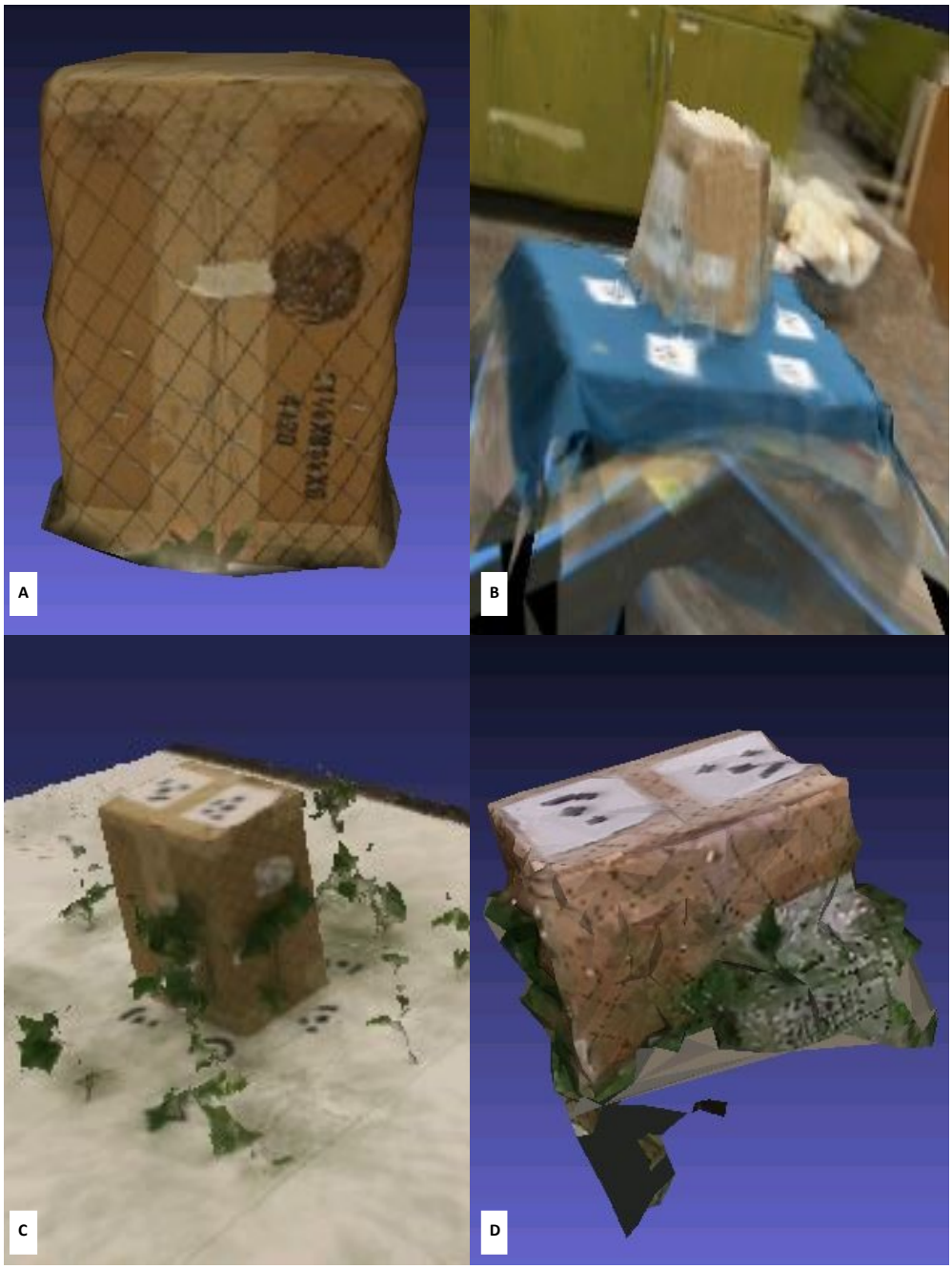

Figure 3.6: Models from the Box study with no vegetation. A) high quality model with low error. B) low quality model with high error. C and D represent the vegetation studies. C) high quality model with vegetation B) low quality model with vegetation.

A comparison between LAI and vegetation obscurity indicates that vegetation obscurity increases with LAI and appears to be non-linear (Figure 3.7). Vegetation obscurity gives a more accurate estimate of the total vegetation coverage of the box when compared to LAI. Therefore, vegetation obscurity should be used to evaluate vegetation effects on a model's accuracy. Figure 3.7 also indicates that there is a relationship between LAI and the vegetation obscurity index.

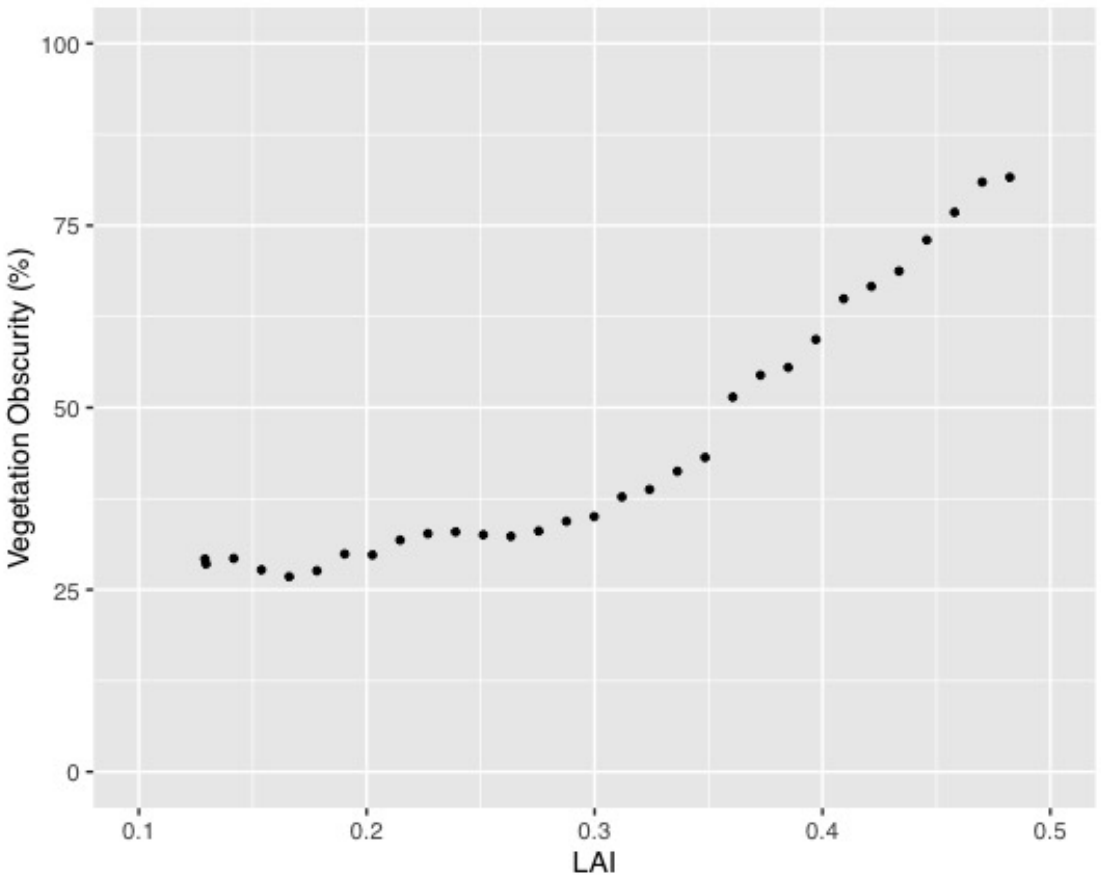

Figure 3.7: LAI compared to vegetation obscurity for the box study. At an LAI greater than 0.35 models accuracy decreases.

3.2 Soil Pyramid Studies

This study focused on how vegetation growth and density could affect SFM (Structure-From-Motion) photogrammetry. The volumes of the truncated pyramids were 0.178 m^3 and 0.95 m^3. A minimum number of images captured for each survey was 40 images for both pyramids. Coded targets were placed around each pyramid as ground control points for volume measurements calculated through Agisoft Photoscan. To understand the relationship between vegetation obscurity and time the obscurity index was used. Table 3.1 shows the relationship of vegetation obscurity index to time.

Table 3.1: Evaluation of Vegetation Obscurity on Pyramid Models.

Week	**Vegetation Obscurity [%]**
0	0
1	21
2	39
3	89
4	100

Results show a correlation between increased vegetation to increased volume error in a pyramid model. As vegetation grew, the mass from the vegetation created a greater volume in 3D reconstruction. The results of this study indicate that increased vegetation increases error within a model (Figure 3.8). SFM was capable of producing models of the pyramids over time as vegetation increased. NRMSE substantially increased at week three, thus reducing accuracy in volume measurements. Camera technologies had similar levels of accuracy throughout the study. After five weeks of growth vegetation had reached 100% obscurity, and after three weeks volume estimation was no longer possible, demonstrating that dense vegetation can effect volume measurements at this scale. Figure 3.9 shows the

models corresponding to vegetation growth over time at each week that vegetation obscurity was evaluated. Each model increases in error over time as vegetation density increases.

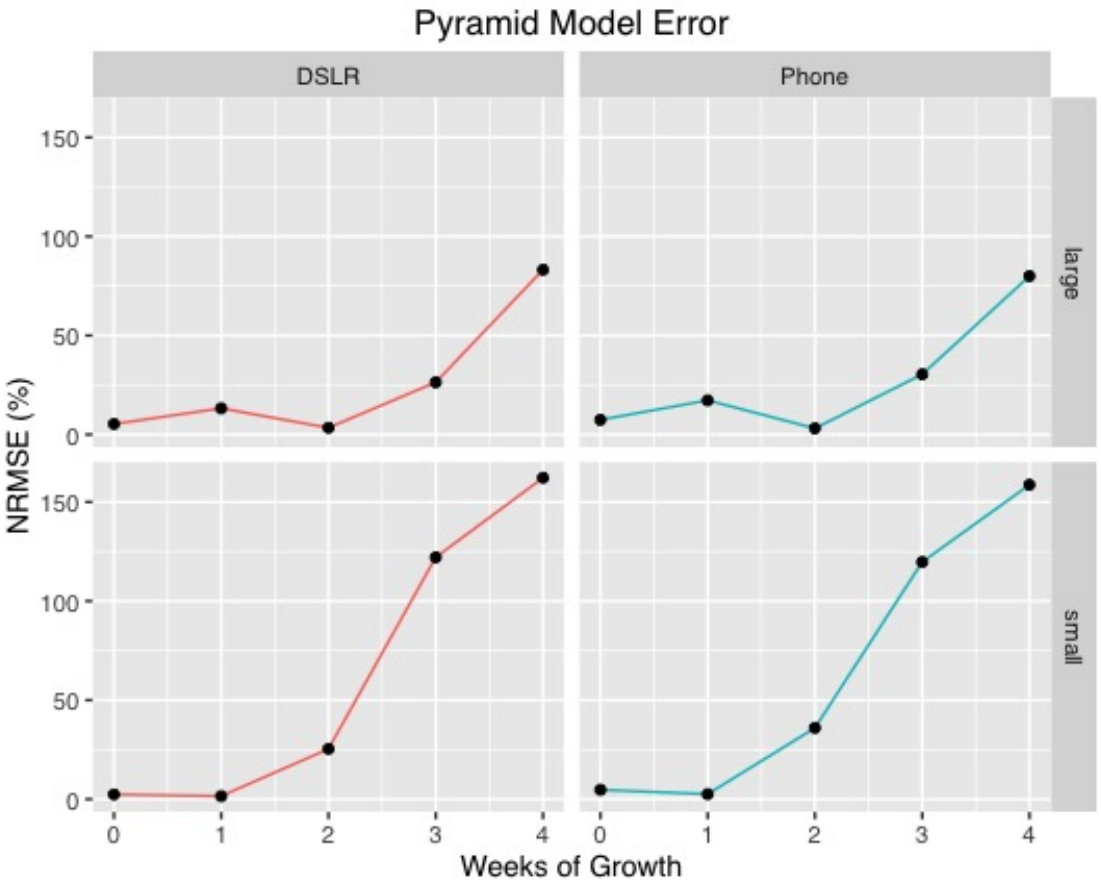

Figure 3.8: Pyramid Study Model From Week 0

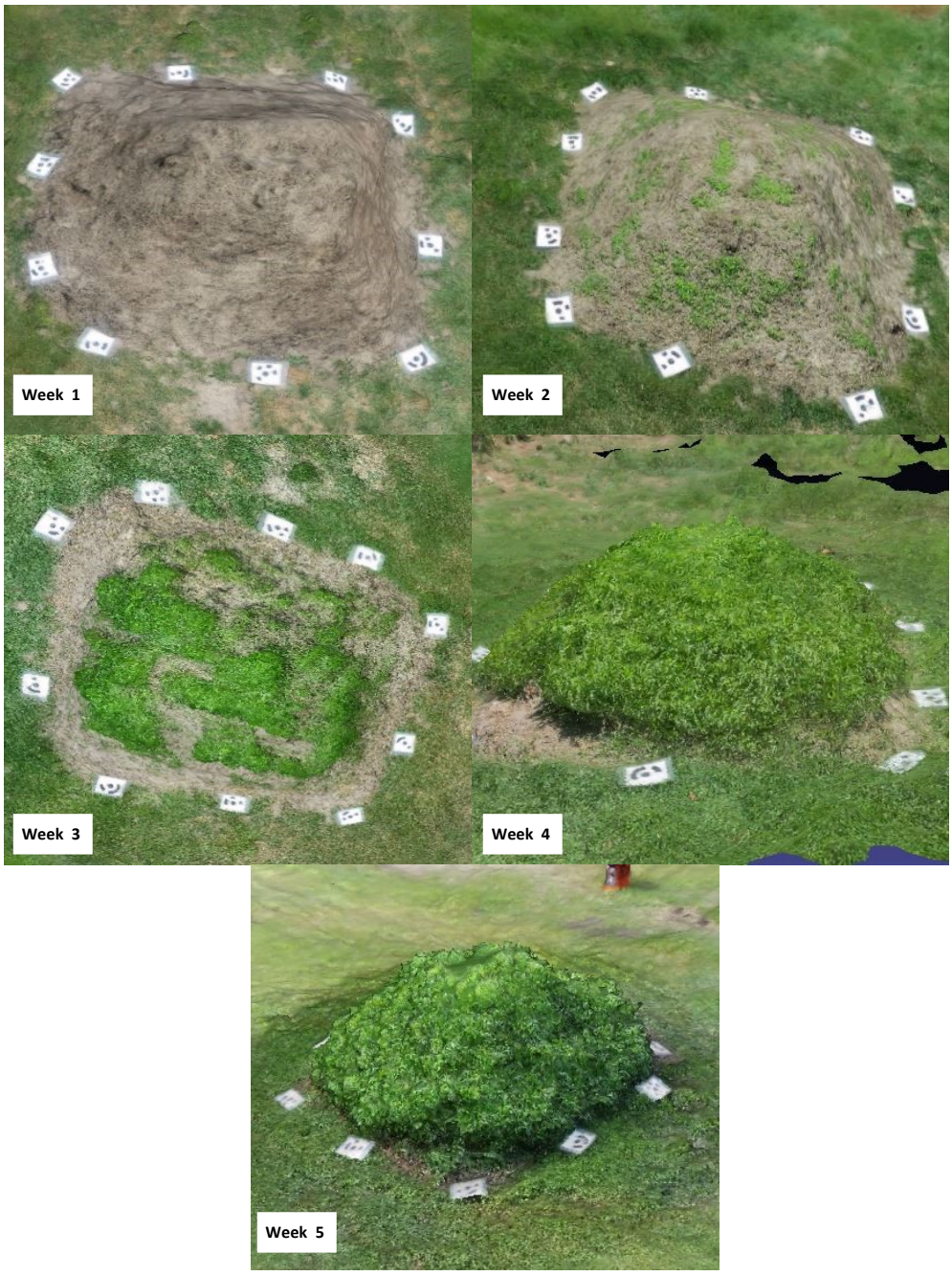

Figure 3.9: Pyramid Study Models From Week 0 to Week 4. Each week represents vegetation growth from zero percent vegetative coverage to 100 percent vegetative coverage. Each model is projected differently due to the interpretation in Agisoft.

3.3 Stream Study

Results from this study showed the capabilities and constraints of using photogrammetry in fluvial geomorphological field work. Based on the elevation differences from a transect survey to corresponding SFM, point NRMSE values were calculated. SFM produced models (DEMs) that were comparable to the transect data. Models were considered accurate when having less than 1.0 m error between survey techniques. Once the baseline study was concluded (total station survey compared to photogrammetry survey 1), results were used from the transect comparison to DEMs of survey 1 for a secondary study to evaluate change over time.

The objective of the baseline study was to compare elevation data from the transect survey to that of SFM survey 1 (Figures 3.10 and 3.11). The comparison maps show the differences between the survey techniques as well as the extent of each survey along the stream bank. DEMs produced a cross-sectional profile of the stream bank surveyed. The cross-section is a multitude of points meshed together spatially, from the images captured with each camera. The points in the DEMs are interpolated and combined together through Agisoft Photoscan from the images and known ground control points.

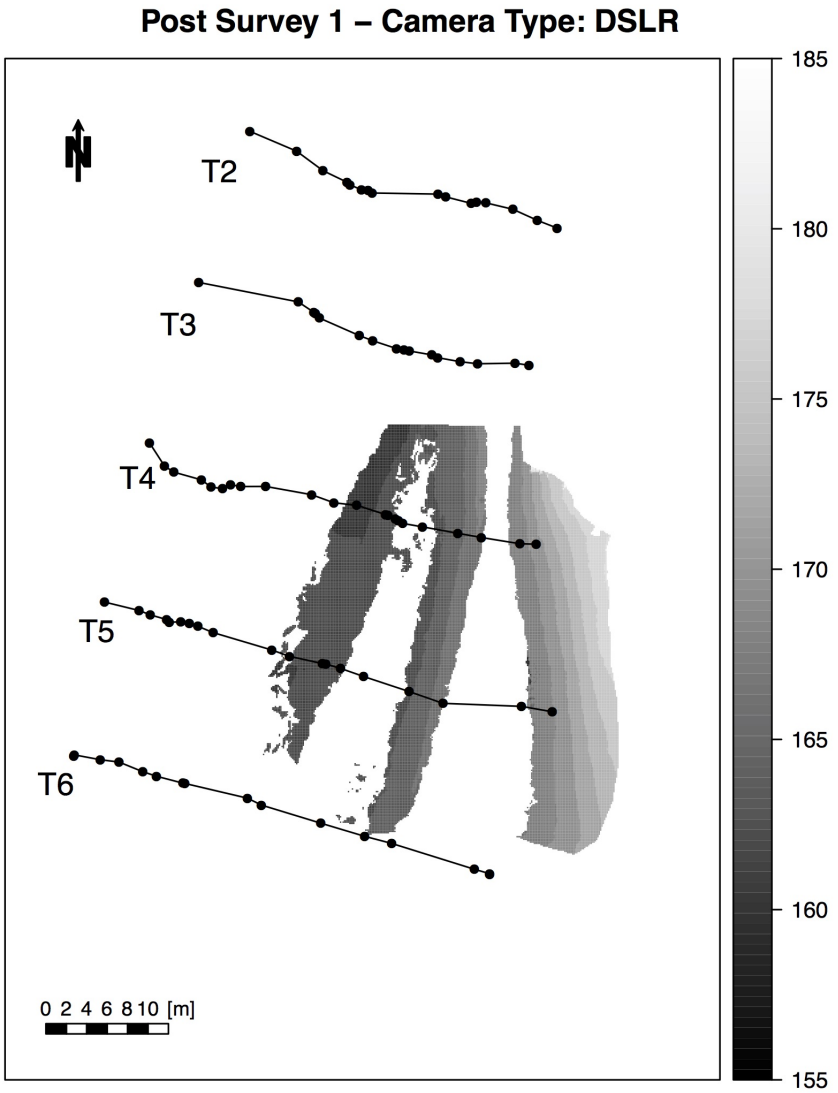

Figure 3.10: Survey 1 map showing the DEM from photogrammetry using a DSLR camera, overlaid with transects from the total station survey.

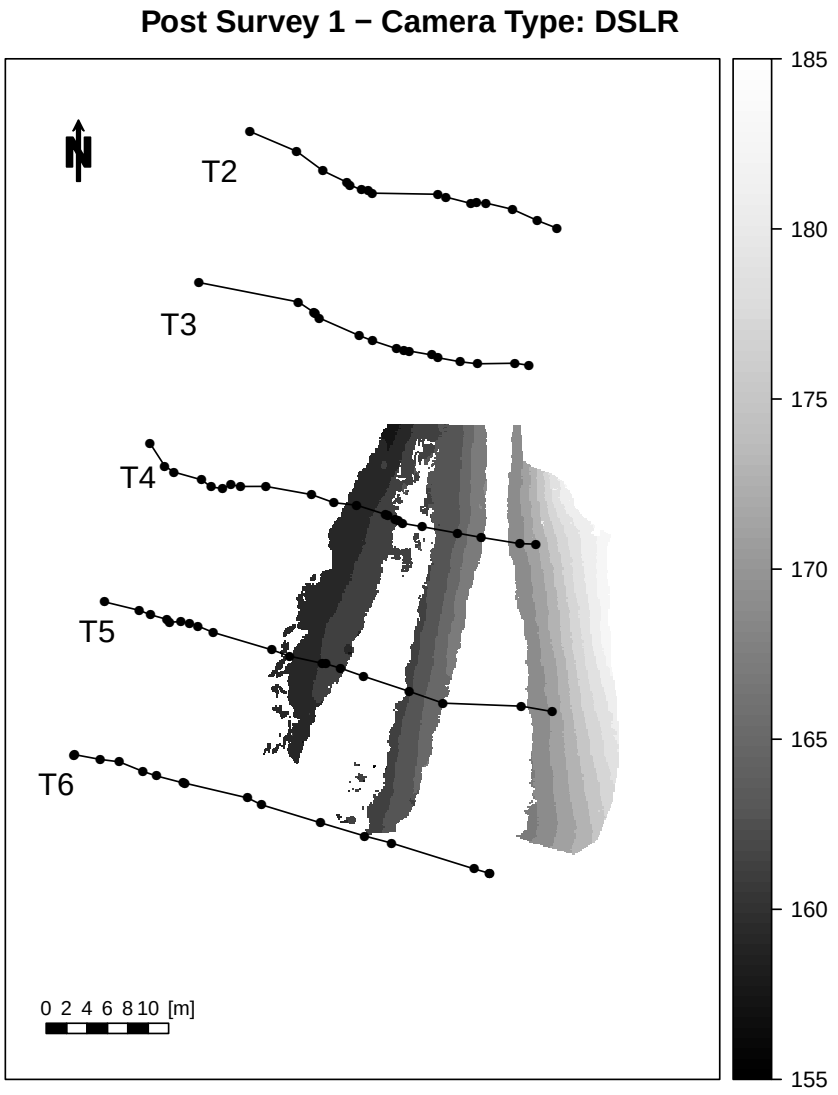

Figure 3.11: Survey 1 map showing the DEM from photogrammetry using a cell phone, overlaid with transects from the total station survey.

Once the models were constructed, they were compared to the total station survey. Results showed each camera was capable of producing a DEM. Overall the RMSE for the comparison was similar in relation to similar studies producing NRMSE values of less than 0.5 m (Dietrich, 2016; Hooke., 1997; Prosdocimi et al., 2015). The results showed the two camera types had similar levels of accuracy having an average NRMSE value of 0.89m for the cell phone and 0.40m for the DSLR. Results indicate that both cameras were capable of reconstruction and monitoring stream geometry change, and both camera types produced accurate models when compared to the transect surveys (Figure 3.12). The summary plot of the transect and SFM survey shows three lines, representing the stream bank surveyed. The lines each have dashed portions representing areas of the bank outside of the camera view and the solid line represents what the cameras were able to capture. However, with a transect survey points are connected and interpolated for distances and slopes to determine measurements of the stream bank. The plot indicates that the lines are very similar and show how accurate a SFM model can be in relation to a total station survey.

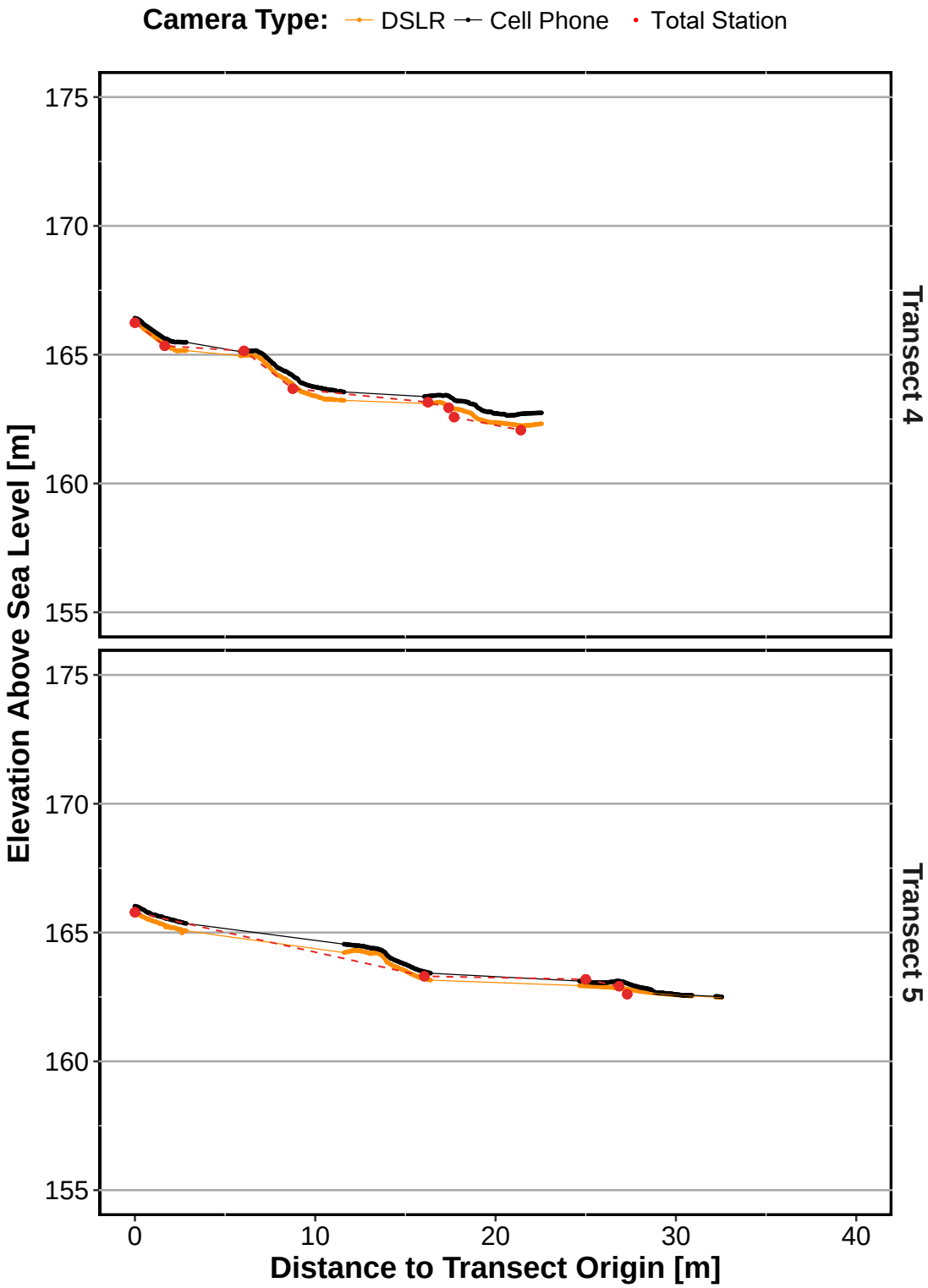

Figure 3.12: The plot shows the difference in elevation between the transect survey and SFM survey. Top: transect 4, bottom: transect 5. Camera techniques were also evaluated for accuracy compared to the total station technology. The plot indicates that both camera technologies had similar outputs when compared to the total station transects.

3.3.1 DEM Comparison Over Time

Elevation changes over time were evaluated between DEMs when compared to survey 1 and survey 12. Figure 3.13 and 3.14 represent models of high quality and poor quality. The model produced through Photoscan are important as a visual aid in understanding where error may come from in each model. The results for the models are shown in Figures 3.15 comparison to survey 1, and 3.16 comparison to survey 12. The results indicate that error over time was sporadic and not a defined pattern of increase or decreased error. In fact, DEMs were very similar and did not seem to change drastically over time . The few models that did seem to increase in error were the DEMs from surveys 6DSLR, 9Phone, and 10DSLR. Standard error maps showing change over time were created to show where along the study area the greatest elevation differences were. Each camera had similar results as indicated from the maps (3.17 and 3.18). Standard error maps show that the closer the ground surface was to the camera the lower the error a DEM elevation contained. This suggest that both camera technologies were similar in accuracy and both were capable of monitoring stream change over time. Results can also provide information on success of stream restoration efforts. As there was little change in DEMs elevation over time, the stream was shown to be stable and able to withstand outside pressures.

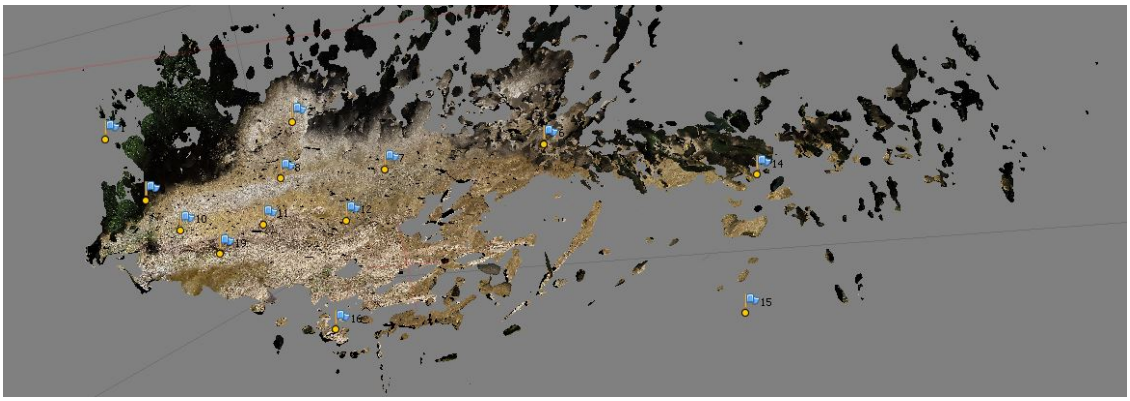

Figure 3.13: A low quality model produced through Agisoft Photoscan.

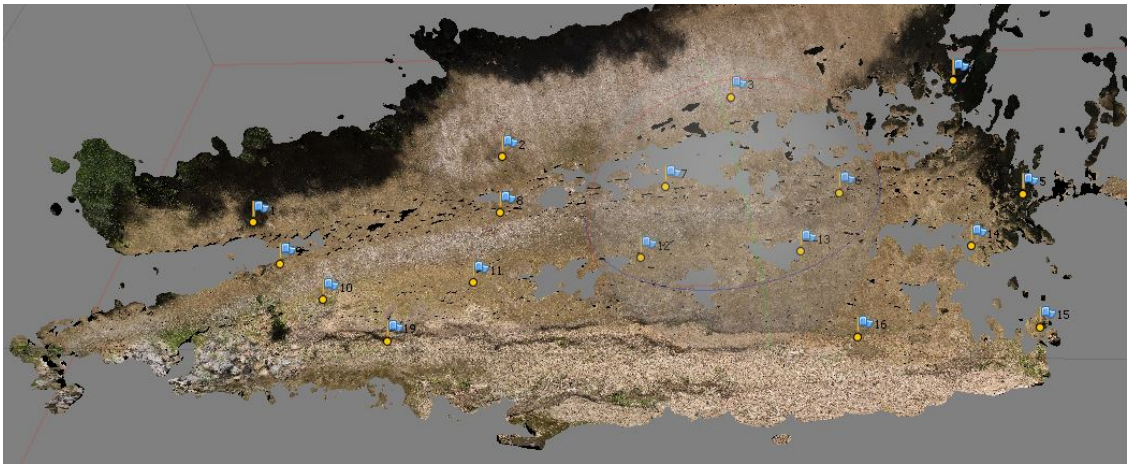

Figure 3.14: A high quality model produced in Agisoft Photoscan.

As indicated in Figures 3.15 and 3.16 there are several models that stand out. To understand the models that stood out the reports generated from Agisoft were analyzed. Reports from Agisoft give an overall summary of model production. The error in models were created due to several key factors: GCP recognition, shadowing, and ability of camera technology to capture the entire scene. The reports indicated that each of the models with outliers had greater error in GCP (ground control point) accuracy, and image recognition. DEMs from surveys 6DSLR, 9Phone, and 10DSLR each had one ground control point with large spatial error of greater than a few meters. GCP accuracy plays a key role in the accuracy of a DEM. As for the rest of the surveys, all GCPs had high accuracy of less than a meter in error. Figure 3.15 and 3.16 show that each of the models with low error in GCPs have low error when compared to surveys 1 and 12. Surveys 4 and 6 were outliers having a greater error between models; these models had greater error among all GCPs and image recognition than other models. Image recognition is important for creating models with photogrammetry; without quality image recognition models become obscure. Figure 3.13 and Figure 3.14 show a model of high quality and a model of poor quality. The high error in models 9cellphone and 10DSLR were created from poor accuracy of GCP 1. Each model having poorly defined DEMs had higher error in GCPs. To prevent error in GCPs each GCP must be placed by hand in the center of the target, as this will decrease overall error in DEM

projection. Each of the obscured models lacked sufficient images of a specific target or lacked proper image overlap to properly construct DEMs. Survey dates and weather conditions are provided in appendix C (Table C.1).

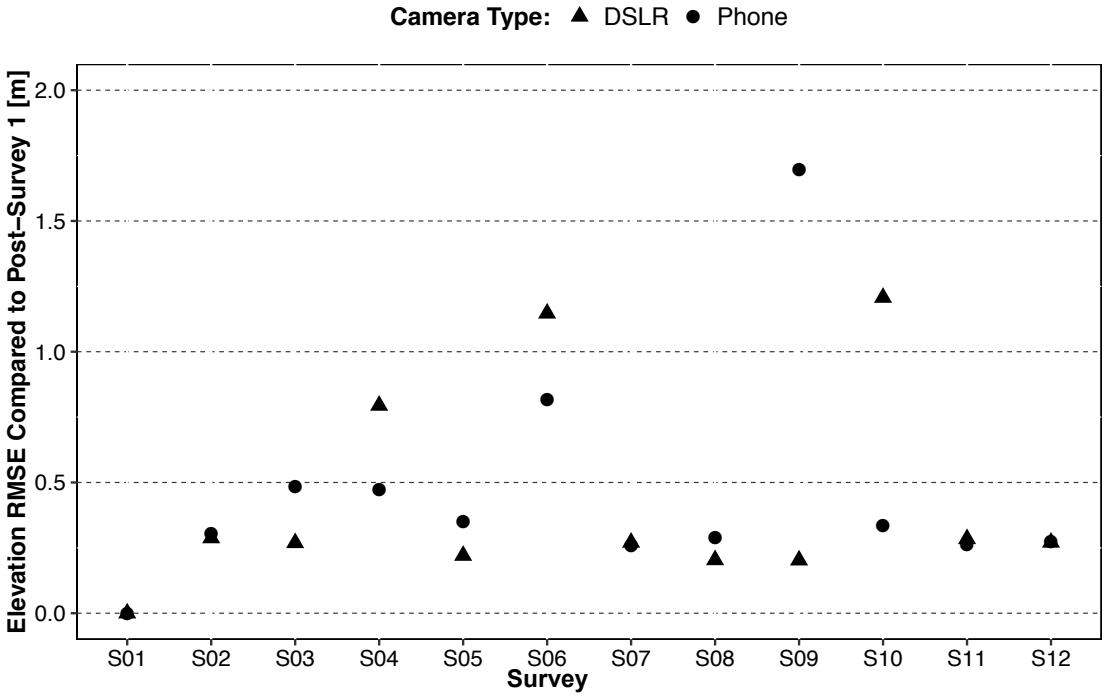

Figure 3.15: DEMs from each post-survey compared to Survey 1. RMSE values are low and show little change over time . Although only slight elevation changes were detected, the camera technologies were similar in accuracy.

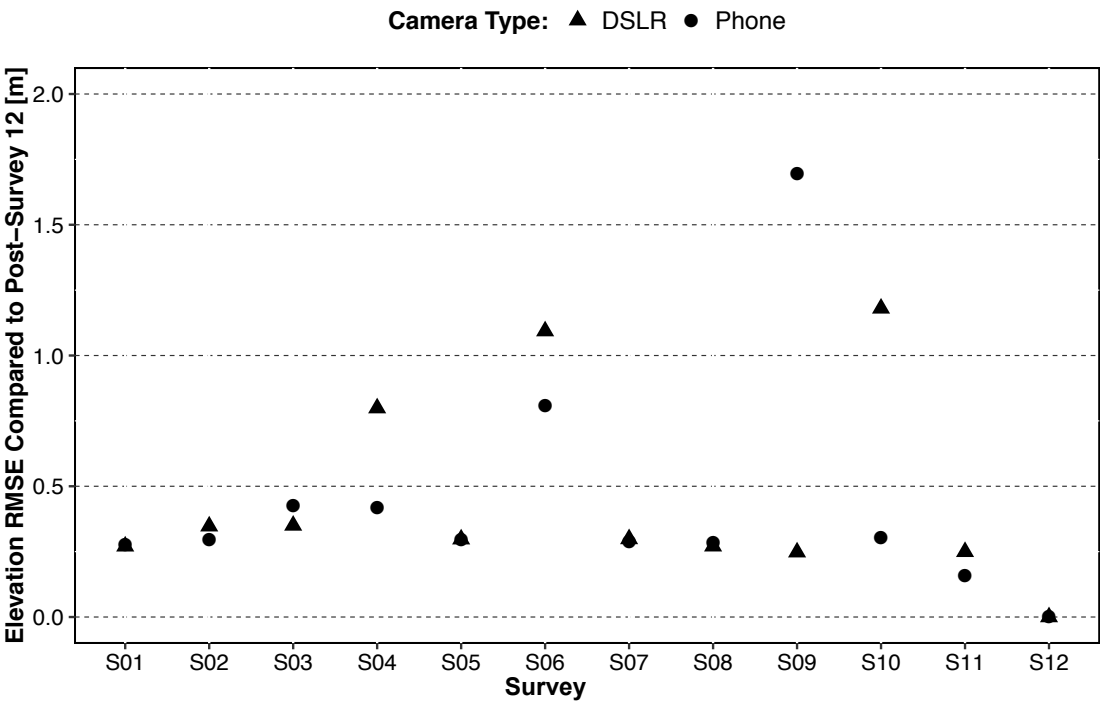

Figure 3.16: DEMs from each post-survey compared to survey 12. RMSE values are low and similar to that of the comparison to survey 1. Although only slight elevation changes were detected, the camera technologies were similar in accuracy.

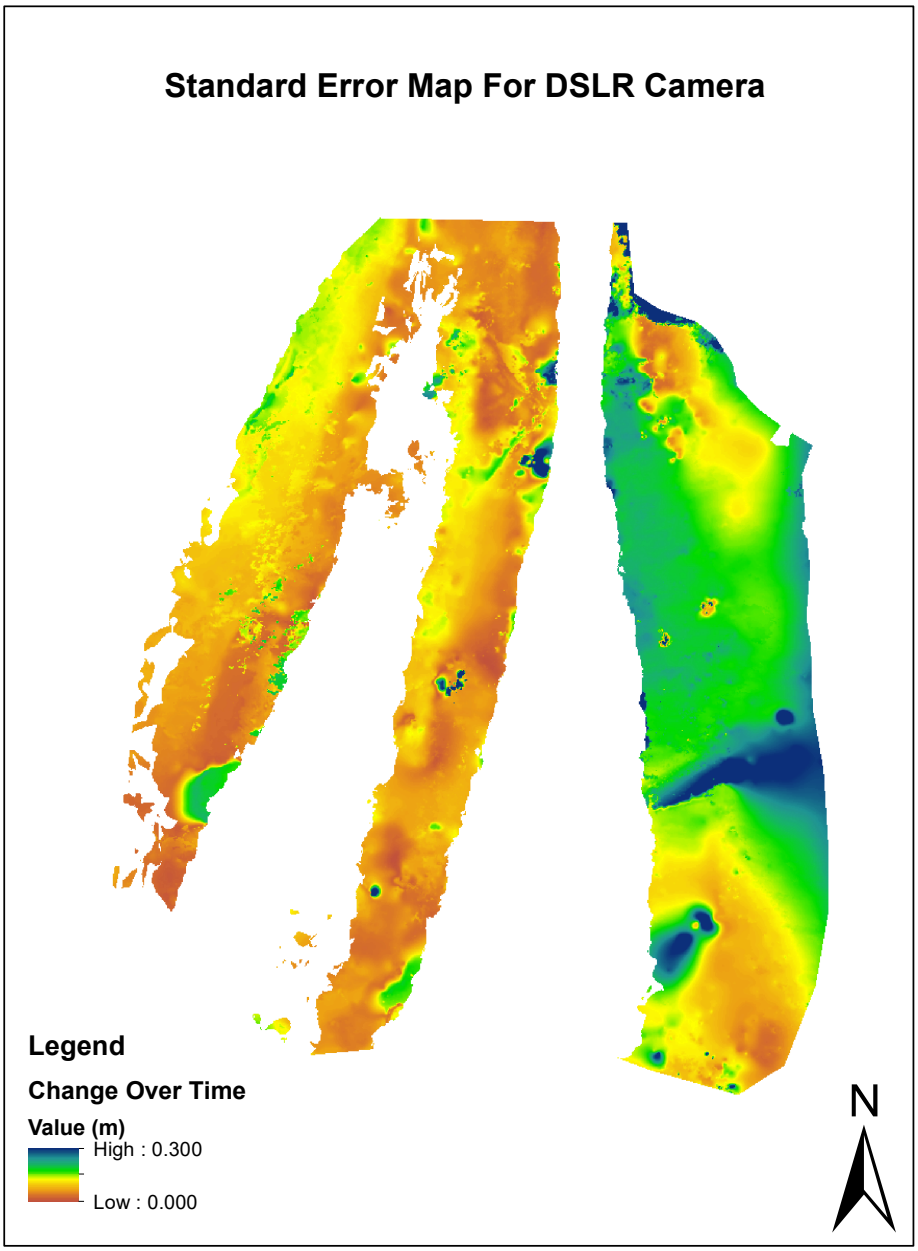

Figure 3.17: Standard Error Map showing elevation differences when compared with DSLR camera technology. Standard error map shows that land surface closer to the camera is more accurate. The figure shows the distribution of values from the models produced with DSLR technology. Areas in orange and red are contain low error, and areas in green and blue have high error.

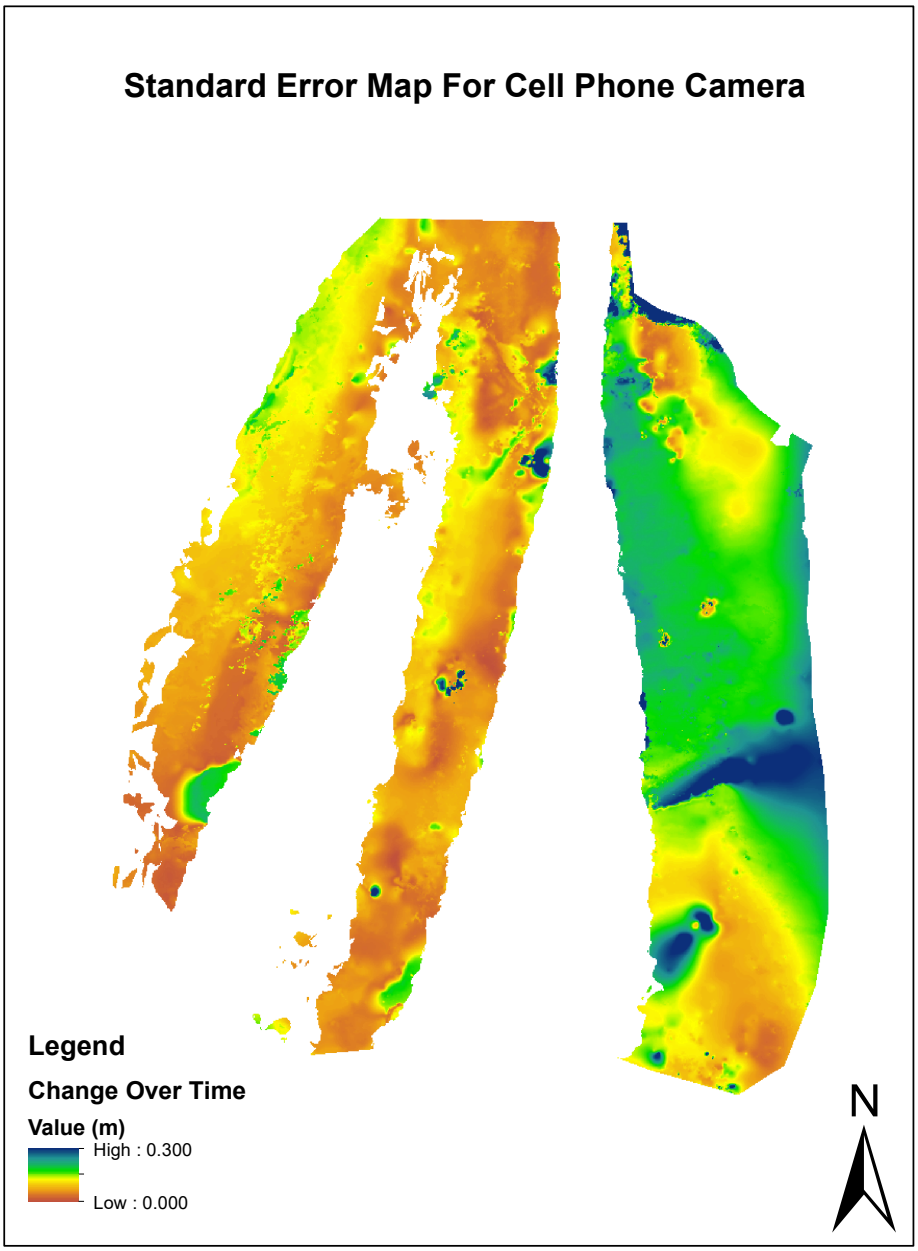

Figure 3.18: Standard Error Map showing elevation differences when DEMs compared to cell phone technology. Standard error map shows that land surface closer to the camera is more accurate.The figure shows the distribution of values from the models produced with cell phone technology. Areas in orange and red are contain low error, and areas in green and blue have high error.

Chapter 4

Discussion

Structure from motion has the capabilities of producing high quality models through 3D image reconstruction. From small scale controlled studies (box study) to field controlled studies of the soil pyramids and uncontrolled field studies, SFM was capable of producing high quality 3D models. Throughout the study models had varying degrees of success based on several factors such as number of photos, angle at which photos were taken, quality of photos, and obscurities (Lane, 2000; Westoby et al., 2012). SFM in this study was tested for accuracy based on number of photos and obscurities such as vegetation.

Smaller scale photogrammetry studies are necessary to understand how the SFM process and software work. Controlled studies are a crucial part for camera calibration and gathering information on possible research questions or objectives (Westoby et al., 2012). The box and pyramids studies were both important for understanding how SFM worked. The controlled studies evaluated the capabilities and constraints of SFM by assessing the following: the number of photos, angle of photo capture, and vegetation effects on models. It was necessary to understand these parameters before larger scale studies were conducted (Westoby et al., 2012). Findings of the box and pyramid studies provided understanding of the capabilities and constraints of the SFM software Agisoft Photoscan.

The application of SFM methods provides similar results in comparison to the traditional total station survey as shown in previous studies (James and Robson, 2012; Westoby et al., 2012; Fonstad et al., 2013). The ability to create photogrammetric models of Parkerson Mill Creek restoration project was successful for all surveys. Areas that were hard to model included areas above the bank and flat areas that the camera could not capture. Models with large gaps were not meshed together properly, likely due to the height at which the images

were taken and GCP recognition. Photogrammetry is a cost effective method for creating 3D models and making measurements. The use of photogrammetry has greatly increased throughout fields of science such as geomorphology, history, and agriculture (Dietrich, 2016; Teichertc., 2008). The new technology allows users to create 3D reconstructions through images, as well as make measurements from output data in Agisoft. Although photogrammetry could be used as a tool for monitoring streams and reconstruction of other objects, there are several constraints. Issues such as dense vegetation, GCPs accuracy, canopy cover (shading) and height at which images were taken all contributed to the error of a model's reconstruction and measurements (Lane, 2000; Armistead, 2013; Dietrich, 2016).

When evaluating topographic survey methods for cost, effort, and accuracy, SFM is a method that is low cost, low effort, and has the potential for high accuracy (Table 4.1). Table 4.1 list the overall differences between each survey technique used throughout the study. The total station data was provided by the City of Auburn, (TOPCON, 2017) and (Agisoft, 2016). Total station and SFM are very different survey methods. Total station survey is based on point to point measurements, while SFM creates a DEM, which is a multitude of points stitched together. Both survey methods can be accurate if used under the right conditions. This study focused on a point to point comparison; however, SFM produces many more points that were not evaluated. SFM studies should address the capabilities of SFM collectively using the entire DEM produced to evaluate accuracy (objective 2).

SFM can be applied to many disciplines for making measurements. Its cost, ease of use and accuracy make it an economically friendly survey method. As describe throughout this study, SFM Produced models at various scales in an advantageous way based on cost effort and accuracy. SFM was capable of measuring stream changes over time when compared to total station and when compared to baseline studies. When using SFM, several parameters must be met, such as: GCPs placement and recognition, camera field of view, and even lighting. If these parameters are met, SFM can be a powerful tool for surveying

and making measurements. If all parameters are met SFM can be a powerful tool for making measurements and surveying.

In conclusion SFM DEMs were accurate and were able to produce data to evaluate change over time. Cameras technologies were also evaluated based on accuracy of data collection and DEM resolution. Based on the results both camera technologies had success in creating accurate DEMs, results also indicates that cameras may not be the reason for errors among models. Agisoft Photoscan also produces model reports with details of each model such as DEM quality, resolution, error in markers and camera calibration. The majority of the error among models was the marker placement (GCPs). Marker placement is a tedious task during the process of creating models, markers are used as reference data that ties all points together. As from the reports models that had greater error in DEMs had a larger error in GCPs.

Table 4.1: Comparison of Survey Methods

Survey Method	**Spatial Resolution (no. points per m)**	**Estimated Cost ($)**	**Effort (Man-hours)**	**Resolution (cm or m)**
Total Station	.1-5	3,000-15,000	16 Field Hours 2 Data analysis Hours	cm
SFM	100s-100,000	549-3,499	1 Field Hours 2 Data Analysis Hours	m

4.1 Data Collection Constraints

A plan around goals or objectives is essential when conducting a photogrammetry survey. This ensures necessary parameters are met for scene reconstruction. It is important to have sufficient image overlap (60%) to accurately describe the scene to be reconstructed. Without proper image capture, Agisoft Photoscan as well as other image software is unable to correctly recognize a relationship among images. The same applies if images are blurry or not of good quality, which also prevents point cloud estimation (Fonstad et al., 2013). Furthermore,

to georeference and make measurements of a scene, ground control points are important. At least three GCP's should be in every modeled scene. Maintaining camera height and angle are also important for accurate reconstruction of a study area. The above parameters enhanced Agisoft Photoscan's ability to reproduce an accurate model. Furthermore, a set height, camera angle, non-blurry images, and a large number of GCPs, in a survey increase the overall quality of Agisoft Photoscan models.

4.2 Photogrammetry and Total Station Data Comparisons

To evaluate DEMs, a point to point comparison was made between the total station data and the photogrammetry data. The values observed were extracted from the DEM to compare to a single point in the transect survey. The differences in the two surveys were calculated using the normalized RMSE, concluding that the values for the SFM survey were similar to that of the total station data. On average the SFM surveys produced an average NRMSE value less than 1m for both camera types. The SFM data set has a much higher resolution than the total station survey, and the data is generated through interpolation of the surface model created in Agisoft, with minimal photographic and GPS coordinate data inputs.

There were potential sources of error within the data sets from the DEMs. Factors leading to error could be shading, vegetation, and camera height. The vantage point for image capture was low (1.8m) from the ground, playing a significant role in the ability for the models to be reproduced without having a lot of blank spaces. The blanks in the models were caused by the camera not being able to capture the whole area within a single image. The camera could only capture what it could see, therefore, the higher elevations in topography created problems in model reconstruction. Thus, the SFM models (DEMs) had holes which created problems when projecting the DEMs and comparing data.

A point to point comparison is a sufficient way to directly compare total station to SFM data, but this method of comparison does not focus on the primary advantage of SFM

reconstruction. SFM generates much more data and at much higher resolution than that data of a total station survey; The data set provided much more detail than that of the total station data.

It is important to note this study focused not only on the comparison of survey techniques but that SFM is capable of producing much more than a two-dimensional line of data points. Hooke. (1997) also stated that photogrammetric modeling could detect a greater amount of change within a stream bank such as volume which is spatially variable and can not be picked up by transect surveys. The DEMs produced from photogrammetry were detailed, but with the use of a second survey methods such as GPS these models could become accurate (Hooke., 1997; Baptiste et al., 2016).

4.2.1 Evaluation of Stream Change

A secondary study was conducted comparing DEMs of each survey to the first and last surveys in the SFM study. The data from this study explains stream change over time. When comparing the DEMs to the first survey, the RMSE should increase, showing change or natural degradation and widening. However, when comparing the DEMs to the last survey there should be a decrease in RMSE showing a reverse pattern of degradation and widening. Having several methods to understand channel evolution is important in understanding how a stream responds to outside pressures. This is important information when stream restoration is necessary. Stream restoration aims to restore streams to a stable state, taking in considerations of outside pressures such as extreme flows.

Chapter 5

Conclusion and Recommendations

SFM was able to produce DEMs which show changes in observed points. Furthermore, this study had high levels of success for monitoring and detecting change within fluvial systems. SFM offers much more flexibility among stream geometry surveys; however, it is not an outright replacement for traditional methods. Future studies should focus on camera positioning and vegetation affects such as shading on photogrammetric models. This study surveyed vegetation year round; however, Lane (2000) suggest that photogrammetry surveys be conducted in dormant low vegetation seasons.

This study points out the constraints and capabilities for SFM photogrammetry at three different scales. At a LAI of 0.07, model accuracy decreases and repeatability becomes an issue with SFM surveys in the field. Vegetation plays a major role in obscuring models created with SFM, as the box studies and pyramid studies show that, as vegetation increases, NRMSE among models significantly increased (objective 1). This study focused on how vegetation affects SFM models. Previous studies also conclude that vegetation could be the sole issue of varying accuracy in models (Lane, 2000; Armistead, 2013). Vegetation plays a major role in obscuring a model; as concluded from the box study, a LAI of 0.07, decreased models accuracy. The same conclusion was reached within the pyramid study; as vegetation grew and became more dense, the error among models increased significantly. When vegetation was added each model increased in volume, therefore, the model had error due to vegetation growth. Vegetation could have been an issue for less accurate models in the stream study, as those models had greater NRMSE values. The vegetation also created shading in some models produced, leading to DEMs varying in size and shape.

This study provides information on the constraints of SFM with cell phone and digital camera technology. Photogrammetry orthophotos and DEMs provide important information for monitoring the riparian vegetation planted as a part of stream restoration (Armistead, 2013). Westoby et al. (2012) and (James and Robson, 2012) indicated that SFM photogrammetry is comparable to ground base LIDAR if the input requirements for SMF are adequately met. Fonstad et al. (2013) explained it is important to have proper image collection, as blurry images or not enough images can decrease accuracy of 3D reconstruction. Furthermore, this study shows that with proper image capture model reconstruction is possible. SFM has the potential to survey stream change and has greater resolution when compared to total station. SFM also has more available data that can be evaluated from SFM surveys (Dietrich, 2016).

Lastly this study looked at replication over time (objective 3) . SFM models were consistent over time having similar extents and sizes. Each DEM produce was accurate and functional for comparison. The majority of the DEMs were very similar as the results indicated, therefore, SFM is considered an accurate method for measuring stream geometry changes.

5.1 Recommendations for Future Work

To improve accuracy within this study several factors must be evaluated. These factors include: camera height, GCPs, total station surveys, and size of 3D reconstruction. The cameras used were unable to capture all of the topography within the survey area. Therefore, repeatability is uncertain and all DEMs produced were missing sections of the survey site. By using a longer camera pole to take images from a greater vantage point, the surveys could increase in accuracy and produce a full extent DEM (Armistead, 2013). Another factor leading to error in the model's accuracy were GCPs. To increase accuracy among GCPs, the GPS unit should have RTK connection and be stabilized for a count longer than 500. This method of GPS collection would ensure accuracy for GCPs, which would increase the accuracy or georeference of the DEMs. For future studies GPS point data or total station

data needs to be acquired for every SFM survey. The data collected from both survey techniques could be used to analyze how these technologies compared over time . This study looked at only one total station survey in comparison to 12 SFM surveys over a seven month period. Lastly, the extent of the survey may have been too large for accurate DEMs to be produced. Micheletti et al. (2015) showed that SFM with DSLR and cell phone technology can be an accurate method to survey riverbank change at less than 10 m. Therefore, the stream study should be divided into smaller sections for a more accurate model.

5.2 Applications for SFM

Results indicated that there are many factors that could decrease SFM accuracy in reproduction. SFM can be used to determine volume measurements of small controlled objects; however, in large uncontrolled settings SFM is more complex. Smaller scene reconstruction of 10 m in length or less should be evaluated for a more reliable data set. SFM at a small scale is an accurate measurement tool, and can be used to survey such things as erosion of small sections of streams and headcuts, where erosion begins and works its way back upstream. Surveying headcuts with SFM would allow a better understanding of stream erosion. The method of SFM in this study was shown to be a tool that can be used to monitor change over time. With accurate GCPs, moderate vegetation, better camera visibility, and evenly dispersed lighting, SFM can be an accurate tool for making measurements. SFM is a relatively new method for 3D surveying, and by using these methods laid out here as well as other studies, SFM can be an accurate 3D survey method.

Appendix A

R Script Steps

A.0.1 Transect and DEM comparison

The following steps were used in R to evaluate the difference between the transect survey and SFM survey 1.

1. Imports sampling data and Creates Lines for Individual Transects.
2. Creates shapefile with individual sampling sites - all transects confounded
3. Converts Points to Polylines
4. Imports raster data and Extract Raster Values
5. Creates datasets to store results for plotting
6. Iteration over individual survey methods
7. Create data to compare Elevation measurements to DEM estimations
8. Comparison of elevation between DEM models and GPS data
9. Extract elevation values at individual sampling sites
10. Elevation Data across Transects
11. Extract raster values along individual transects (lines), Associates each sampling location to a cell number and creates a data frame
12. Associate cell numbers along individual transects to X,Y coordinates
13. Exports results

14. Transfer results to final datasets

15. End for loop over survey methods

16. Computes RMSE

17. Plot Results

The following steps were used to create a map comparison between the transect survey and SFM survey.

1. Imports Shapefiles, Converts to Polyline, and Formats Data

2. Creates shapefile with individual sampling sites - all transects confounded

3. Converts Points to Polylines

4. Import Rasters and Plot maps

5. Iteration over individual raster files

6. Imports Raster File

7. Defines file name for individual plots

8. Generates plots and save as jpeg

9. End iteration over individual raster files

10. End iteration over sub-directories

A.0.2 DEM Comparison Over Time

The R script steps below was used to compare surveys over time to evaluate channel evolution.

1. Determination of Study Area

2. Import Study Area Outmost Boundary
3. Set work directory
4. Import study area outmost boundary from polygon shapefile and Define Projections as WGS84 UTM 16N
5. List all Mesh DEMs used to Determine Study Area
6. List DEMs
7. Crop DEMs to Outmost Boundary Extent and Resample (Resolution = 5cm)
8. Create list where re-sampled mesh DEMs will be stored
9. Import and Resample Mesh DEMs
10. Import mesh DEM from raster file
11. Crop mesh DEM to the Outmost Boundary Extent
12. Convert non-NAs mesh DEM values to 1
13. Create list where resampled mesh DEMs will be stored
14. Set all raster values different than NA to 1
15. Superpose Mesh DEMs
16. Determine Study Area and Export Result
17. Crop Point Cloud DEMs to Determined Study Area
18. Import mesh template
19. List all Point Cloud DEMs
20. Crop Point Clouds DEMs to Mesh Template and Export Results

21. Compute Models RMSE

22. Plot Data

23. Compute SE map

24. Create Matrices containing all DEM values

25. Compute Standard Error for Each Raster Pixed

26. Create Rasters with Standard Error

27. Export Data

Appendix B

Random Box Study Vegetation Placement

Table B.1: Random Model Trials.

Trial	**Quadrant**
1	17, 24
2	10
3	16
4	16
5	41
6	47
7	33
8	28
9	4
10	34
11	17
12	44
13	24
14	36
15	7
16	33
17	30
18	19
19	41
20	27
21	9
22	4
23	14
24	3
25	35
26	26
27	5
28	11
29	2
30	35
31	28
32	32

Table B.2: Random Model Trials.

Trial	**Quadrant**
33	0
34	7
35	43
36	22
37	15
38	3
39	32
40	41
41	30
42	24
43	35
44	25
45	46
46	16
47	28
48	32
49	44
50	21
51	10
52	29
53	18
54	16
55	6
56	43
57	8
58	11
59	20
60	28
61	31
62	34
63	8
64	10
64	22

Appendix C

Stream Survey Dates and Weather Conditions

Table C.1: Stream Survey Dates and Weather Conditions

Survey	Date	Weather Data
1	3/16/16	Scattered Clouds
2	4/08/16	Clear
3	4/29/16	Clear
4	5/16/16	Clear
5	5/26/16	Scattered Clouds
6	6/08/16	Clear
7	6/24/16	Scattered Clouds
8	7/12/16	Partly Cloudy
9	7/24/16	Scattered Clouds
10	8/17/16	Clear
11	9/18/16	Mostly Cloudy
12	9/29/16	Clear

* Weather data provided by Weather Underground:https://www.wunderground.com (The Weather Company, 2018).

Bibliography

Agisoft. *Agisoft PhotoScan User Manual*. Agisoft Photoscan, professional eddition 1.2 edition, 2016. URL `http://www.agisoft.com/pdf/photoscan-pro_1_2_en.pdf`. Accessed 12-August-2016.

C. C. Armistead. *Applications of Structure from Motion Photogrammetry to River Channel Change Studies*. PhD thesis, Boston College. College of Arts and Sciences, 2013.

ASPRS. *Manual of Photogrammetry*. The American Society for Photogrammetry and Remote Sensing (ASPRS), 6 edition, 2016.

E. S. Australia. Geometry and dynamics of stream channels, 2016. URL `http://earthsci.org/flooding/unit3/u3-01-01.html`.

D. Baldocchi. Lectures 3 characterizing the vegetation on canopy, part ii: Leaf area index. Technical report, University of California at Berkeley, Ecosystem Science Division, 2012.

W. Ballow. The evaluation of measuring stream channel morphology using unmanned aerial system based structure from motion photogrammetry. *Geosciences Theses*, Aug. 2016.

M. Baptiste, V. Damia, C. Gibbins, and D. R. Ramon, Batallaand Green. Application of structure-from-motion photogrammetry to river restoration. *Earth Surface Processes and Landforms*, Apr. 2016.

T. J. Beechie, D. A. Sear, J. D. Olden, G. R. Pess, J. M. Buffington, H. Moir, P. Roni, and M. M. Pollock. Process-based principles for restoring river ecosystems. *BioScience*, 60(3): 209–222, Mar. 2010.

E. S. Bernhardt, M. A. Palmer, J. Allan, G. Alexander, K. Barnas, S. Brooks, J. Carr, S. Clayton, C. Dahm, J. Follstad-Shah, et al. Synthesizing us river restoration efforts. *Science*, 308(5722):636–637, 2005.

J. A. J. Berni, P. J. Zarco-Tejada, L. Suarez, and E. Fereres. Thermal and narrowband multispectral remote sensing for vegetation monitoring from an unmanned aerial vehicle. *IEEE Transactions on Geoscience and Remote Sensing*, 47(3):722–738, Mar. 2009.

S. Bird, D. Hogan, and J. Schwab. Photogrammetric monitoring of small streams under a riparian forest canopy. *Earth Surface Processes and Landforms*, 35(8):952–970, June 2010.

B. Blizard. The art of photogrammetry: introduction to software and hardware, 2014. URL `http://www.tested.com/art/makers/460057-tested-dark-art-photogrammetry`. (Accessed 22-Jan-2017).

D. B. Booth and C. J. Fischenich. A channel evolution model to guide sustainable urban stream restoration, 2015.

N. J. J. Bréda. Ground-based measurements of leaf area index: A review of methods, instruments and current controversies. *Journal of Experimental Botany*, 54(392):2403–2417, Jan. 2003.

J. M. Chen and T. A. Black. Defining leaf area index for non-flat leaves. *Plant, Cell Environment*, 15(4):421–429, May 1992.

S. Clarified. Floodplain, April 2003. URL `http://www.scienceclarified.com/landforms/Faults-to-Mountains/Floodplain.html`. (Accessed 01-March-2017).

A. Clewell, J. Rieger, and J. Munro. Guidelines for developing and managing ecological restoration projects. Technical report, Society of Ecological Restoration, Tucson, 2000. URL `http://web.archive.org/web/20041029153203/http://www.ser.org/content/guidelines\_ecological\_restoration.asp`.

R. Conniff. Rebuilding the natural world: A shift in ecological restoration. *Yale Environment 360*, 2014.

R. Copeland, D. McComas, C. Thorne, P. Soar, M. Jonas, and J. Fripp. Hydraulic design of stream restoration projects, 2001.

DataStar. What every researcher should know about statistical significance, 2008.

L. M. De Santisteban, J. Casalí, and J. J. López. Assessing soil erosion rates in cultivated areas of navarre spain. *Earth Surface Processes and Landforms*, 31(4):487–506, Apr. 2006.

P. E. Debevec. *Modeling and Rendering Architecture from Photographs*. PhD thesis, University of California at Berkley, 1996.

J. T. Dietrich. Riverscape mapping with helicopter-based structure-from-motion photogrammetry. *Geomorphology*, 252:144–157, Jan. 2016.

B. Dikovski, P. Lameski, E. Zdravevski, and A. Kulakov. Structure from motion obtained from low quality images in indoor environment, 2016.

B. A. Doll, G. L. Grabow, K. R. Hall, J. Halley, W. A. Harman, G. D. Jennings, and D. E. Wise. *Stream Restoration: A Natural Channel Design Handbook*. NC Stream Restoration Institute, 2003.

M. A.-B. Ebrahim. Using mobile phones digital cameras in close range photogrammetry, 2004.

T. A. Endreny. Classifying stream equilibrium. Technical report, State University of New York :Environmental Resources Engineering, 2016.

M. L. Erwin and P. A. Hamilton. Monitoring our rivers and streams, August 2005. URL `https://pubs.usgs.gov/fs/fs-077-02/`. (Accessed 03-May-2017).

H. Fawzy. The accuracy of mobile phone camera instead of high resolution camera in digital close range photogrammetry. *International Journal of Civil Engineering and Technology (IJCIET)*, 6(1):10, 2015.

M. A. Fonstad, J. T. Dietrich, B. C. Courville, J. L. Jensen, and P. E. Carbonneau. Topographic structure from motion: A new development in photogrammetric measurement. *Earth Surface Processes and Landforms*, 38(4):421–430, Mar. 2013.

S. J. F. C. N. D. S. Gloss and E. Bernhardt. River and riparian restoration in the southwest: Results of the national river restoration science synthesis project. *Restoration Ecology*, 15 (3):550–562, 2007.

Á. Gómez-Gutiérrez, S. Schnabel, F. Berenguer-Sempere, F. Lavado-Contador, and J. Rubio-Delgado. Using 3d photo-reconstruction methods to estimate gully headcut erosion. *Catena*, 120:91–101, Sept. 2014.

N. R. Haney and L. Davis. Potential controls of alluvial bench deposition and erosion in southern Piedmont streams, Alabama (USA). *Geomorphology*, 241:292–303, July 2015.

B. Hargreaves. Accuracy and precision, 2017. URL `http://bhargreaves.com/2012/05/accuracy-precision/`. (Accessed 23-May-2017).

S. Holmes. Rms error, Nov. 2000. URL `http://statweb.stanford.edu/~susan/courses/s60/split/node60.html`. (Accessed 23-March-2017).

R. B. L. D. J. Hooke. Use of photogrammetry for monitoring and measuring stream bank erosion. *Earth Surface Processes and Landforms*, 1997.

M. R. James and S. Robson. Straightforward reconstruction of 3d surfaces and topography with a camera: Accuracy and geoscience application. *Journal of Geophysical Research: Earth Surface*, 117(F3):F03017, Sept. 2012.

L. Javernick, J. Brasington, and B. Caruso. Modeling the topography of shallow braided rivers using structure-from-motion photogrammetry. *Geomorphology*, 213:166–182, May 2014.

S. JMO. Worldwide historical estimates and bibliography of leaf area index. *ORNL Technical Memorandum*, 2001.

R. F. Keim, A. E. Skaugset, and D. S. Bateman. Digital terrain modeling of small stream channels with a total-station theodolite. *Advances in Water Resources*, 23(1):41–48, Sept. 1999.

C. Kidson and M. Manton. Assessment of coastal change with the aid of photogrammetric and computer-aided techniques. *Estuarine and Coastal Marine Science*, 1(3):271, 1973.

J. Kim, S. Lee, H. Ahn, D. Seo, S. Park, and C. Choi. Feasibility of employing a smartphone as the payload in a photogrammetric UAV system. *ISPRS Journal of Photogrammetry and Remote Sensing*, 79:1–18, May 2013.

P. LaFlamme. Introduction to dynamic equilibrium. Technical report, Vermont Rivers Program and Dynamic Equilibrium, 2011.

P. S. Lake. On the maturing of restoration: Linking ecological research and restoration. *Ecological Management & Restoration*, 2(2):110–115, Aug. 2001.

S. N. Lane. The measurement of river channel morphology using digital photogrammetry. *The Photogrammetric Record*, 16(96):937–961, Oct. 2000.

S. N. Lane, K. S. Richards, and J. H. Chandler. Developments in photogrammetry; the geomorphological potential. *Progress in Physical Geography*, 17(3):306–328, Jan. 1993.

S. N. Lane, K. S. Richards, and J. H. Chandler. Developments in monitoring and modelling small-scale river bed topography. *Earth Surface Processes and Landforms*, 19(4):349–368, June 1994.

S. Lee, J. Kim, C. Jin, S. Bae, and C. Choi. Assessment of smartphone based technology for remote environmental monitoring and its development. *Instrumentation Science and Technology*, 40(6):504–529, Nov. 2012.

L. Leopold and T. Maddock. The hydraulic geometry of stream channels and some physiographic implications. *Department of the Interior*, 252:1–64, 1953.

N. Matthews. Aerial and close range photogrammetric technology: Providing resource documentation, interpretation, and preservation, 2008.

K. J. McCree and J. H. Troughton. Non-existence of an optimum leaf area index for the production rate of white clover grown under constant conditions. *Plant Physiology*, 41 (10):1615–1622, 1966.

J. C. McGlone and G. Y. G. Lee. *Manual of Photogrammetry*. American Society for Photogrammetry and Remote Sensing, Bethesda, Md., 2013. ISBN 978-1-57083-099-0.

M. F. Merigliano. Hydraulic geometry and stream channel behavior: A uncertain link. *JAWRA Journal of the American Water Resources Association*, 33(6):1327–1336, Dec. 1997.

W. K. T. Meyer.J.L, Michael J. Paul. Stream ecosystem function in urbanizing landscapes. *Journal of the North American Benthological Society*, 24(3):602–612, 2005.

N. Micheletti, J. H. Chandler, and S. N. Lane. Investigating the geomorphological potential of freely available and accessible structure-from-motion photogrammetry using a smartphone. *Earth Surface Processes and Landforms*, 40(4):473–486, Mar. 2015.

NRCS. Urban soil erosion and sediment control. Technical report, USGS, 2008.

NRCS. Natural channel and floodplain restoration, applied fluvial geomorphology, 2010.

S. K. Pandey and H. Singh. A simple cost effective method for leaf area estimation. *Journal of Botany*, 2011:e658240, Nov. 2011.

M. A. Perez, W. C. Zech, and W. N. Donald. Using unmanned aerial vehicles to conduct site inspections of erosion and sediment control practices and track project progression. *Transportation Research Record: Journal of the Transportation Research Board*, 2528:38–48, Jan. 2015.

G. Pess, T. Beechie, J. Williams, D. Whitall, J. Lange, and J. Klochak. Watershed assessment techniques and the success of aquatic restoration activities. *American Fisheries Society*, pages 185–201, 2003.

M. Prosdocimi, S. Calligaro, G. Sofia, G. Dalla Fontana, and P. Tarolli. Bank erosion in agricultural drainage networks: New challenges from structure-from-motion photogrammetry for post-event analysis. *Earth Surface Processes and Landforms*, 40(14):1891–1906, Nov. 2015. WOS:000363702200004.

P. Reich and P. S. Lake. Extreme hydrological events and the ecological restoration of flowing waters. *Freshwater Biology*, 60(12):2639–2652, Dec. 2015.

D. L. Rosgen. A classification of natural rivers. *Catena*, 22(3):169–199, June 1994.

J. Ross. *The Radiation Regime and Architecture of Plant Stands*. Springer Netherlands, Dordrecht, 1981. ISBN 978-94-009-8649-7 978-94-009-8647-3.

RStudio Team. *RStudio: Integrated Development Environment for R*. RStudio, Inc.,, Boston, MA, 2015.

A. M. Samad, A. Ahmad, and N. Ishak. Assessment of digital camera for mapping stream using close range photogrammetric technique. In *International Colloquium on Signal Processing and Its Applications (CSPA)*, volume 6, pages 1–5, May 2010.

M. Satchet. Feasibility study of using mobile phone camera in digital close range photogrammetry. *Journal of Thi - Qar University*, 7(1):10, 2011.

M. Scherer and J. Luis Lerma. From the conventional total station to the prospective image assisted photogrammetric scanning total station: Comprehensive review. *Journal of Surveying Engineering-Asce*, 135(4):173–178, Nov. 2009. WOS:000270914300006.

K. Schindler. Math of photogrammetry. *Photogrammetry and Remote Sensing*, 2016.

S. M. H. Schumm and C. Watson. Incised channels: Morphology, dynamics, and control. *Water Resources Publications*, page 200, 1984.

D. A. Sear. River restoration and geomorphology. *Aquatic Conservation: Marine and Freshwater Ecosystems*, 4(2):169–177, June 1994.

C. T and R. Draxler. Root mean square error (rmse) or mean absolute error (mae)- arguments against avoiding rmse in literature. *Geosci. Model Dev*, 7(3):1247–1250, 2014.

R. Taylor. *An Introduction to Error Analysis: The Study of Uncertainties in Physical Measurements*. University Science Books, 1997.

G. G. A. E. B. Teichertc. The photogrammetric potential of low-cost uavs in forestry and agriculture. *The International Archives of the Photogrammetry, Remote Sensing and Spatial Information Sciences*, 36:1207–1214, 2008.

The Weather Company. Weatherunderground, 2018. URL `https://www.wunderground.com/history/airport/KAUO/2016/9/29/DailyHistory.html?req_city=&req_state=&req_statename=&reqdb.zip=&reqdb.magic=&reqdb.wmo=`. (Accessed 12-April-2018).

Topcon. Total station. Internet, 2017. URL `https://www.topconpositioning.com/en-na/product-launcher`.

TOPCON. Reflectorless total stations. topconpositioning.com, May 2017. (Accessed 15-November-2017).

M. Weiss and F. Baret. Methods for leaf area index determination part i: Theories, techniques and instruments. *Department of Land management*, page 42, 2016.

M. J. Westoby, J. Brasington, N. F. Glasser, M. J. Hambrey, and J. M. Reynolds. 'structure-from-motion' photogrammetry: A low-cost, effective tool for geoscience applications. *Geomorphology*, 179:300–314, Dec. 2012.

J. Wiens. Spatial scaling in ecology. *Functional Ecology*, 3(4):385–397, 1989.

J. Williams. Accuracy vs. precision...know the difference?, 2017. URL `http://blog.wheaton.com/accuracy-vs-precision-know-the-difference/`. (Accessed 08-June-2017).

G. Yan, R. Hu, Y. Wang, H. Ren, W. Song, J. Qi, and L. Chen. Scale effect in indirect measurement of leaf area index. *IEEE Transactions on Geoscience and Remote Sensing*, 54(6):3475–3484, June 2016.